Advances in Colloid and Interface Science 335 (2025) 103351

Contents lists available at ScienceDirect

Advances in Colloid and Interface Science

journal homepage: www.elsevier.com/locate/cis

# Polymer-based collectors in flotation: A review

Patrycja S. Bednarek [a], Jan Zawala [b], Przemyslaw B. Kowalczuk [a,*]

[a] Norwegian University of Science and Technology, Department of Geoscience and Petroleum, S. P. Andersens veg 15a, 7031 Trondheim, Norway
[b] Jerzy Haber Institute of Catalysis and Surface Chemistry, Polish Academy of Sciences, 30239 Krakow, Poland

ARTICLE INFO

*Keywords:*
Flotation
Collector
Polymer
Mineral separation

ABSTRACT

Flotation, as a beneficiation process, stands as a foundation in mineral and metal production, handling approximately 70–80 % of the world's exploited ore annually. However, numerous challenges emerge prior to beneficiation, such as the declining quality of ore, necessitating further liberation. This deterioration results in higher energy, water, and reagent consumption. A froth flotation chemicals market analysis reveals an anticipated growth of around 30 % in the next five years, signaling a concerning trend due to the frequent toxicity associated with these chemicals. With increasingly stringent environmental regulations, there is a pressing need to explore more sustainable and non-toxic solutions. Polymers play a significant role in mineral processing as either depressants, flocculants or dispersants. The potential of natural green polymers in these capacities is actively being studied. This review delves into the relatively novel use of polymers as collectors, examining their performance and adsorption mechanisms. Among the papers reviewed, collectors formulations based on either natural or synthetic non-toxic polymers have emerged as environmentally friendly alternatives to traditional collectors. The utilization of polymers opens possibilities for creating nanoparticles, conventional polymers, temperature-responsive polymers and block copolymers with functionalities tailored for specific separation processes. These polymers have shown promising results, achieving recoveries and grades comparable to or better than conventional collectors. Additionally, they could address the challenge of declining ore quality, effectively handling finely ground particles and slimes. Properties such as those in temperature-responsive polymers can be used not only to induce hydrophobicity but also to allow the recycling of the collector for future applications.

## 1. Introduction

The chemical technology of flotation has been well known for over 100 years. Its evolution is reflected in the development of diverse chemical reagents. Despite declining ores and water quality, as well as the need for more innovative and sustainable approaches, the industry's adoption rate of technological improvements remains slow [1].

Flotation reagents typically fall into three categories: collectors, modifiers, and frothers, each playing a crucial role in complex flotation systems. Collectors consist of two distinct structural modules: a functional group containing donor atoms or ligands, along with a hydrophobic substituent group featuring alkyl aryl hydrocarbon chains. The main function of a collector is to selectively form a hydrophobic layer on targeted mineral surfaces within the flotation pulp, allowing these hydrophobic particles to attach to air bubbles and be recovered in the froth product. Frothers are primarily surface-active compounds with both polar and nonpolar regions that reduce water's surface tension and adsorb at the air bubble-water interface. Modifiers, on the other hand, adjust the collector's effect by either enhancing or reducing the hydrophobic properties of mineral surfaces, thereby increasing the collector's selectivity for specific minerals [2–5].

A wide range of organic polymers are utilized in the mineral industry as flotation agents, serving specific modifying roles like depressants, dispersants, or flocculants [6]. According to the classification of flotation reagents presented by Wang [7], a polymer compound can also play a role of a collector. A polymeric collector is a reagent with a structure based on large molecules formed by chemically bonded and repeated monomers, with a molecular weight (determined by the length and arrangement of its molecular chains) tailored to meet desired features specified by manufacturer. Searching databases like Scopus, Web of Science, Scilit, Springer, and ACS Publications using keywords such as 'Polymer', 'Collector', and 'Flotation' has revealed a noticeable increase in attention to the polymer collector topic since the 2000s, with even steeper growth in the last decade (Fig. 1). However, further examination

---

* Corresponding author.
*E-mail address:* przemyslaw.kowalczuk@ntnu.no (P.B. Kowalczuk).

https://doi.org/10.1016/j.cis.2024.103351
Received in revised form 11 November 2024;
Available online 17 November 2024

of results from the Scopus database showed that only 24 % of the studied polymeric flotation reagents actually played a collector role (Fig. 2).

The way polymers adhere to mineral surfaces involves a variety of reactions, both physical and chemical in nature. Key methods of adsorption include hydrophobic association, hydrogen bonding, electrostatic attraction, and chemical bonding [6]. The range of chemical bonds involved in this process encompasses ionic, dispersive (van der Waals), covalent, semipolar, hydrogen, and hydrophobic bonds, as well as their various combinations [5].

Polymers and their ability to flocculate fine particles are widely investigated as a remedy for valuable fines recovery. Combining flocculation with flotation can address the arising problem of fines recoveries. In reviews, Forbes [9] and Asgari et al. [10] demonstrated various methods for floc-flotation of fines. Methods such as polymer floc-flotation [11–14], shear floc-flotation [15], and carrier flotation [16–18] can utilize polymers to enhance performance efficiency by agglomerating fines into larger flocs or aggregates. They described the advantages and drawbacks of these methods, highlighting crucial aspects such as the adsorption of bubbles to flocs, the interaction between flocculants and flotation reagents, and the understanding of the variation in floc properties and their effects on flotation.

Dissolved air flotation (DAF) is another separation process often supported by flocculation, where flocs are removed from the slurry by microbubbles [19,20]. In some cases, bubbles are functionalized with reagents like amphiphilic chitosan [21] which enhances the capture process and improves the separation efficiency. The main forces involved in DAF are gravity, buoyancy, and hydrodynamic drag. Gravity drives the separation process by creating a density difference, while buoyancy, enhanced by attached air bubbles, causes the aggregates, which are lighter than water, to rise to the surface. Hydrodynamic drag slows down the movement of these rising aggregates [22].

In the methods listed above, polymers serve as additional reagents to enhance the separation process. Polymers, when used as collectors, can offer a unique combination of flocculating and collecting abilities, particularly in the form of temperature-responsive polymers [23] or block copolymers which are investigated in this review. Additionally, this review examines two other groups in the new collector role: conventional polymers and polymeric nanoparticles.

Some polymeric collectors can perform a dual role as both collectors and frother. Based on the structural design, the placement of functional groups (i.e. carboxyl) within the polymer matrix affects their ability to foam [24]. However, adding a frother can enhance the separation efficiency. Frothers play multiple functions in the flotation system. They are responsible for froth/foam creation, lowering the surface tension of the pulp, and influencing the behavior of the liquid and gas interfaces [25]. Additionally, frothers improve the degree of gas dispersion, which helps stabilizing the froth and inhibiting bubble coalescence [26]. Frothers significantly improve both the likelihood of particles contacting bubbles and the effectiveness of their attachment [27]. Typically, polymeric collectors are used in combination with frothers to enhance material recovery.

The primary focus of this study is on polymers used as flotation collectors, examining their performance and bonding mechanisms on mineral surfaces. Previous reviews have described the collecting ability of polymers in the flotation process; however, they typically focused on limited categories such as temperature-responsive polymers [23], or nanoparticles [28–31]. Reviews based on nanoparticle performance in ion flotation [28,29] primarily describe nanoparticles with graphene oxide cores and silica nanoparticles [29]. Review on nanoparticles in mineral flotation [30] covers a wide range of nanoparticle types, including polymeric nanoparticles such as polystyrene nanoparticles, lignin nanoparticles, and nanocrystalline cellulose, among others non-polymeric types. In paper [31] nanoparticle collectors are presented as a method to modify mineral surface roughness.

This review presents a comprehensive and updated study on polymers as collectors, discussing the advantages and drawbacks associated with their use in flotation. Furthermore, it explores future perspectives and potential advancements within the field of polymeric collectors.

## 2. Types of polymeric collectors

### 2.1. Conventional polymer (P)

There is a need to explore novel green collectors to facilitate a smoother transition in the flotation chemicals market. While polymers offer a wide array of natural and synthetic compounds, their full

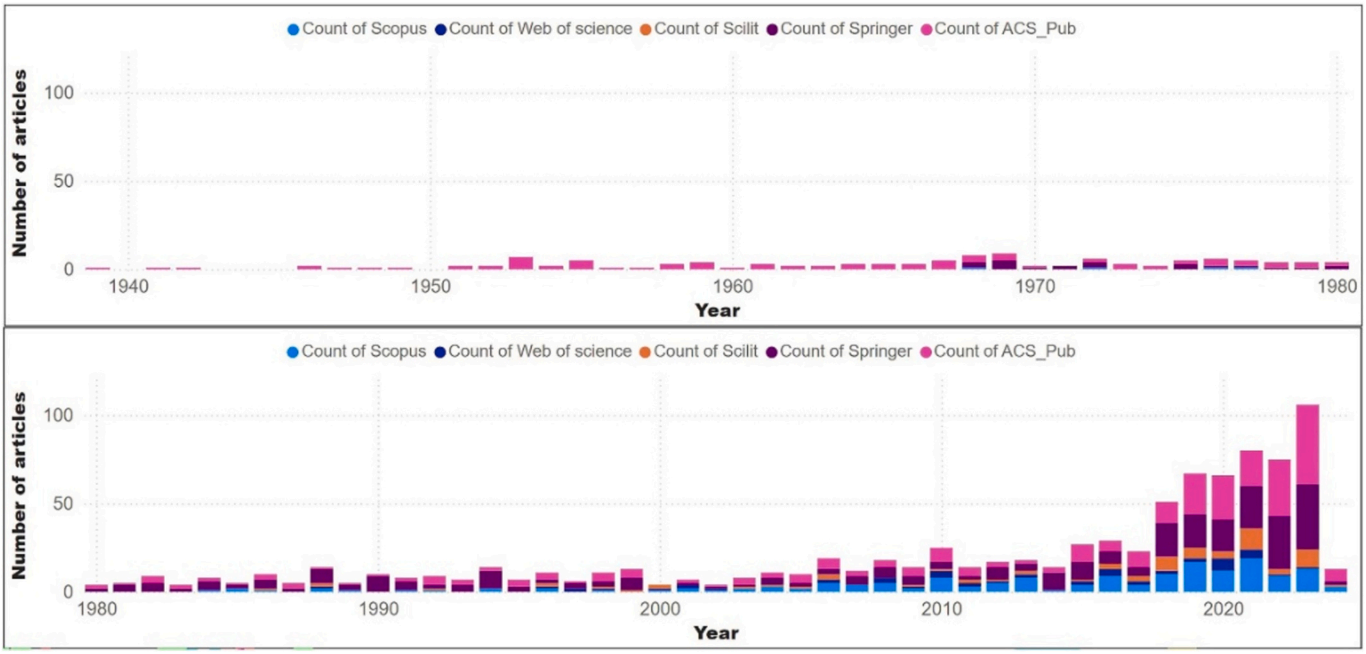

**Fig. 1.** Results of Databases (Scopus, Web of Science, Scilit, Springer, and ACS Publication) Searches Using 'Polymer', 'Collector', and 'Flotation' Keywords, 1938–2024 [8].

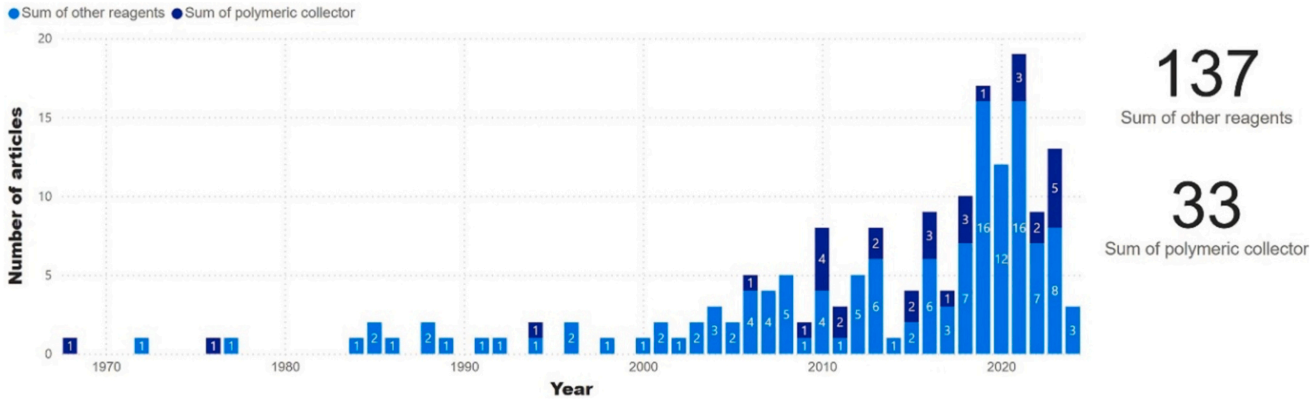

**Fig. 2.** Scopus Search Results for 'Polymer', 'Collector', and 'Flotation' Keywords, Categorized into Polymeric Collectors and Other Reagents, 1968–2024 [8].

utilization in mineral processing has not yet been realized. This chapter presents polymers in their lesser-known role as collectors, demonstrating their potential to compete with conventional chemical reagents. The detailed description of the performance and characteristics of conventional polymers is included in following sections and Table 1.

### 2.1.1. $SiO_2$ derivatives separation

One extensively studied polymer as an environmentally friendly collector is poly(propylene glycol) bis(2-aminopropyl ether) (PEA) [32–35]. According to the Safety Data Sheet for PEA [36], it does not indicate chronic toxicity and does not cause mutations. In the case of quartz separation [32] PEA has demonstrated efficiency at low concentrations and simplifies the reagent scheme during the flotation process, minimizing the use of acids and alkalis. Moreover, PEA showed remarkable results during flotation tests, achieving the quartz recovery at a level of 98 % and feldspar-quartz associated ore (FQA) recovery at only 19 %. These results were obtained with optimized flotation parameters with the particle size of 150–270 μm, PEA concentration $1 \times 10^{-4}$ M and pH 9–9.5. The adsorption mechanism relies on electrostatic and hydrogen bonding between the negatively charged quartz and the $—NH_3^+$ /$—NH_2$ head groups of PEA. Although feldspar is also negatively charged over a wide range of pH (above 1.85), PEA adsorbs less to feldspar due to electrostatic repulsion between the positive K and Na ions and the positively charged amine groups within PEA (Fig. 3).

In paper [33], the authors presented PEA as a possible collector for the recovery of silicon (Si) from photovoltaic industry kerf-loss Si slurry waste. PEA exhibited excellent Si floatability and selectivity in Si-SiC slurry. The maximum recovery of Si, equal to 80 %, and SiC, equal to 91 %, was achieved with a PEA concentration of $5 \times 10^{-6}$ mol/L at pH levels of 2 and 9, respectively. The Si grade can achieve over 92 % at pH 9 in the sinking part of the floated Si - SiC mixture. On the other hand, a SiC grade of around 70 % was achieved at pH 11 in the collected concentrate (from Si – SiC). The separation between Si and SiC under alkaline conditions occurs because the SiC surface is more negatively charged than the Si surface, making SiC more efficient at adsorbing PEA and facilitating flotation separation. Meanwhile, Si powder can react with $OH^-$ ions to form $Na_2SiO_3$, which suppresses its adsorption behavior towards PEA. This difference in behavior is reflected in the high recovery of SiC in the concentrate, while Si shows a high recovery in the sinking product. The conducted surface analysis showed PEA adsorption on Si and SiC surface by hydrogen bonding and electrostatic attraction. The presence of $–NH_2$, $–CH_3$, and $–CH_2$ groups in PEA not only allows it to adsorb onto the mineral surface but also creates a hydrophobic layer that promotes flotation.

Jiang et al. at research [34] studied the influence of PEA chain length on quartz sand flotation. The study showed that increasing the chain length enhances floatability but reduces the collector's water solubility. The presence of X-ray Photoelectron Spectroscopy (XPS) N(1 s) peaks from the two head groups of PEA ($–NH_3^+$, $–NH_2$) on the quartz surface and their further analysis indicates that protonated $–NH_3^+$ (peak at 402 eV) is electrostatically adsorbed onto negatively charged hydroxyl groups ($OH^-$) on the quartz surface. Additionally, $–NH_2$ groups (peak at 399 eV) bind to Si⋯OH through hydrogen bonding, although to a lesser extent (Fig. 4). PEA achieved better quartz recoveries at lower concentrations: at natural pH, PEA-D2000 ($2 \times 10^{-5}$ mol/L) recovered around 100 % of quartz, PEA-D400 ($6 \times 10^{-5}$ mol/L) recovered 95 %, and conventional collector dodecyl amine (DDA, $14 \times 10^{-5}$ mol/L) recovered around 90 %. Additionally, the authors demonstrated that PEA-400 is an effective collector for low-grade quartz sand, successfully separating it into products of different grade levels.

Another utilization for PEA was proposed by Mo et al. [35]. They studied the flotation behavior of glass fiber powder and proposed the mechanism behind the process. The collector PEA-D2000 achieved a recovery rate of 95 % for glass fiber with a low dosage ($6 \times 10^{-5}$ mol/L), outperforming conventional monoamine collectors. Mo et al. also confirmed the results from previous studies [32–34], showing that PEA adsorbs on glass fiber powder through hydrogen bonding and electrostatic interactions between the PEA' amine groups and the negatively charged glass fiber surface.

### 2.1.2. Magnetite separation

Poly(amidoamine) (PAMAM), a hyperbranched polymer, also possesses environmentally benign characteristics and was investigated as a magnetite collector in research [37]. PAMAM achieved similar magnetite recovery results as Aero 704 (a commercial, conventional collector) in the pH range of 2 to 6, slightly worse results (2–3 % lower) in the pH range of 6 to 9, and better results above pH 9. The adsorption mechanism of PAMAM is based on interactions between its inner amide and amine functional end groups and the mineral surface (Fig. 5). This mechanism changes with pH: below pH 5.5, PAMAM's amine groups convert to positively charged ammonium salts; above pH 6, the polar amine groups interact with the negatively charged iron oxide surface; and above pH 9, metal ions can be coordinated by the inner amide groups. The authors concluded that PAMAM is a strong and selective collector for magnetite. This selectivity is further evidenced by its significantly lower recovery rates with other minerals, achieving around 40 % for galena and smithsonite, and only 25 % for sanidine and quartz.

### 2.1.3. Ion separation

Researchers in [38] presented continuous counter-current foam separation as an alternative process to solvent extraction (SX) for gallium ion recovery. They utilized this method on synthetic multi-metal solutions and leaching solutions of zinc refinery residues, with the surfactant role fulfilled by nonionic poly(oxyethylene) nonylphenyl ether (PONPE20). This surfactant is very toxic to aquatic life with long-lasting effects and is suspected of damaging fertility or the unborn child [39].

**Table 1**

The conventional polymers collectors' performance and adsorption characteristics (NG – not given).

| Polymers/ monomers used/ collector MW | Targeted mineral | Adsorption on mineral surface | Separation performance | Conventional performance (comparison) | Zeta potential | Reference |
|---|---|---|---|---|---|---|
| Poly (propylene glycol) bis (2-aminopropyl ether) (PEA)<br>MW = 400 Da | Quartz – from feldspar-quartz associated ore (particle size 150–270 μm) | The PEA is adsorbed on the quartz surface by electrostatic and hydrogen bonding interaction with —$NH_3^+$ /—$NH_2$ head groups, while is less adsorbed on the feldspar surface due to electrostatic repulsion between the $K^+$ / $Na^+$ ions and the positively charged —$NH_3^+$/—$NH_2$ head groups of PEA. | $10^{-4}$ M PEA, pH 9–9.5:<br>Quartz recovery ~98 %*<br>Feldspar-quartz associated ore (FQA) recovery ~19 % | NG | Zeta potential:<br>Quartz + PEA, pH 9–9.5: −45 mV<br>FQA + PEA: −35 mV | [33] |
| PEA<br>MW = 2000 Da | Silicon (Si), silicon carbide (SiC) – artificial mixture with average Si and SiC powder particle size were 2.7 μm and 7.9 μm respectively | The lone pair of electrons from the polar hydrophilic –$NH_2$ group of PEA are attracted to the negative (Si—O—) or neutral Si–OH groups on the Si or SiC surface, forming hydrogen bonds. In the flotation cell, the –$NH_2$ group partially hydrolyzes to produce –$NH_3^+$ ions, promoting hydrogen or ionic bonding with surface –OH groups of SiC or Si. The positive –$NH_3^+$ group is attracted to the negative Si—O— group on the Si and SiC surface through electrostatic and hydrogen bonding. | Floated separately<br>5 × $10^{-6}$ mol/L PEA<br>pH 9:<br>Si recovery ~54 %<br>SiC recovery ~91 %<br>pH 2:<br>Si recovery ~81 %<br>SiC recovery ~73 %<br>Floated as a mixture<br>pH 11:<br>SiC grade in buoyancy part ~70 %<br>Si grade in buoyancy part ~30 %<br>pH 9:<br>Si grade in sinking part~92 %<br>SiC grade in sinking part ~8 % | NG | Zeta potential at pH 2; 9; 11:<br>Si-SiC mixture + PEA: 7; −16; −45 mV<br>SiC + PEA: 5; −18; −44 mV<br>Si + PEA: 10; −25; −52 mV | [33] |
| PEA<br>MW = 230; 400; 2000 Da | Quartz sand (particle size 180–250 μm) | PEA is attached to the quartz surface mainly by electrostatic adsorption, and to a less extent by hydrogen bond adsorption. | natural pH<br>18 × $10^{-5}$ mol/L PEA-230:<br>Quartz recovery ~90 %<br>6 × $10^{-5}$ mol/L PEA—D400:<br>Quartz recovery >95 %<br>2 × $10^{-5}$ mol/L PEA—D2000:<br>Quartz recovery ~100 % | natural pH<br>14 × $10^{-5}$ mol/L dodecyl amine (DDA):<br>Quartz recovery ~90 % | NG | [34] |
| PEA<br>MW = 230, 400, 2000 Da | Glass fiber powder (GFP), $SiO_2$ content around 58 % (particles are micron sized) | PEA is adsorbed onto the surface of glass fiber powder through – -$NH_3^+$/−$NH_2$ groups, primarily by hydrogen bonding, and supplemented by electrostatic adsorption. | natural pH<br>2 × $10^{-5}$ mol/L PEA—D2000:<br>GFP recovery ~95 % | natural pH<br>6 × $10^{-5}$ mol/L DDA:<br>GFP recovery ~88 %<br>6 × $10^{-5}$ mol/L n-octylamine (OTA):<br>GFP recovery ~90 %<br>6 × $10^{-5}$ mol/L n-butylamine (BTA):<br>GFP recovery ~65 % | Zeta potential at pH 7:<br>GFP + PEA-D2000: −14 mV<br>GFP + DDA: −0.5 mV<br>GFP + OTA: −3 mV<br>Zeta potential at pH 8:<br>GFP + BTA: −40 mV | [35] |
| Poly(amidoamine) (PAMAM) | Magnetite – pure magnetite, quartz and sanidine were selected from rhyolite ore under microscope (particle size 38–106 μm) | Amine functional end groups and inner amide groups can form a complex with metal ions. The magnetite-PAMAM interactions occurred via the inner amide groups of PAMAM above pH 9.5, and at the other pHs, it happens with tertiary and primary amine groups. When pH is above 6, the amine groups of PAMAM are polar and can interact with the negatively charged iron oxide surface. | 1200 g/t of PAMAM, at pH 8:<br>Magnetite recovery ~88 %<br>Sanidine recovery ~25 %<br>Quartz recovery ~25 %<br>1200 g/t of PAMAM, at pH 9:<br>Galena recovery ~42 %<br>Smithsonite recovery ~39 % | 1200 g/t of Aero704, at pH 8:<br>Magnetite recovery ~90 %<br>300 g/t of Aero3000C, at pH 8:<br>Sanidine recovery ~86 %<br>Quartz recovery ~89 % | Zeta potential at pH 8:<br>magnetite + PAMAM: -75 mV<br>magnetite + Aero704: −80 mV | [37] |

(*continued on next page*)

**Table 1** (*continued*)

| Polymers/ monomers used/ collector MW | Targeted mineral | Adsorption on mineral surface | Separation performance | Conventional performance (comparison) | Zeta potential | Reference |
|---|---|---|---|---|---|---|
| Poly(oxyethylene) nonylphenyl ether (PONPE) | Ga(III) – from synthetic multi-metals solution with GA(III), Fe (III), Cu(II) and Zn(II) | PONPE20 affinity towards Ga(III) ions. | 0.1 wt% PONPE20:<br>Ga(III) recovery ~100 %<br>Fe(III) recovery ~1.5 %<br>Cu(II) and Zn(II) recovery <0.5 % | Solvent extraction (SX) with PONPE10:<br>Ga(III) recovery ~71 %<br>Fe(III) recovery ~1 %<br>Cu(II) and Zn(II) recovery ~0 % | NG | [38] |
| PONPE | Au(III) – synthetic multi-metals solution with Au(III) and Cu(II) | PONPE20 affinity towards Au(III) ions. | 0.1 wt% PONPE20:<br>Au(III) recovery ~100 % | NG | NG | [41] |
| β-Cyclodextrin (CD) with Phtalic anhydride, 3-nitrophtalic anhydride | Cu(II) – from synthetic solution | Metal ions react with deprotonated hydroxyl groups of b-CD molecules to be chelated. With pH increase they form more stable chelate complexes. | Frother: $2 \times 10^{-4}$ M Nona(ethylene glycol) ether,<br>20 mg β-CD polymer/100 $cm^3$,<br>pH 5.5<br>3-nitrophtalic linker:<br>Cu(II) recovery ~93 %<br>Phtalic linker:<br>Cu(II) recovery ~73 % | NG | NG | [42] |

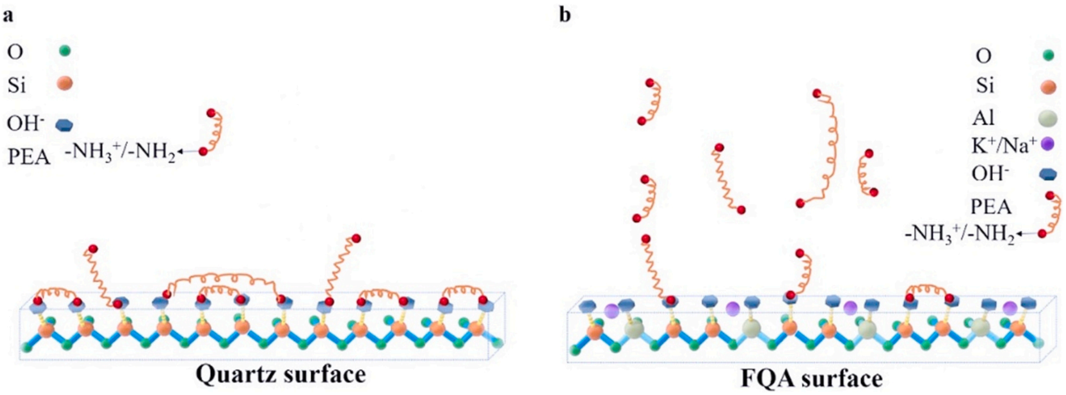

**Fig. 3.** A schematic illustration of conceptual adsorption of PEA cationic collector on quartz (a) and FQA (b) surfaces. Based on [32].

However, the authors suggest this organic solvent-free method is a promising "greener" alternative to traditional SX.

In their research, the authors demonstrated that PONPE20 plays a dual role as both a frother and a metal collector. Continuous counter-current foam separation achieved better separation of Ga(III) from Fe (III) compared to SX or conventional foam separation. A 100 % recovery of gallium ions was achieved from both an artificial metal mixture and a diluted leaching solution with the addition of ascorbic acid. The solvent extraction method achieved a lower recovery rate of 71 % for the latter [38].

In one of their previous work, Kinoshita et al. [40] described the adsorption mechanism of PONPEs with metal ions. Polyoxyethylene nonylphenyl ethers (PONPEs) contain ethylene oxide (EO) units, where the oxygen atoms, due to their electron-donating nature, form complexes with various solutes similarly to how solvating extractants operate. PONPEs exhibit notably high selectivity for gold and gallium over most other heavy metals.

Kinoshita et al. [41] also utilized PONPE as a gold(III) collector for continuous counter-current foam separation. They investigated the effect of average foam diameter and column size on the separation performance. The liquid holdup, i.e. foam diameter, is a crucial factor during separation. Smaller foam (the foam diameter below 0.075 cm) resulted in lower separation efficiency but high recovery, while larger foam (the foam diameter around 0.28 cm) showed the opposite trend. The Au(III) recovery reached 100 %, and the separation factor for Au (III)/Cu(II) was also high around 1060, with the Cu(II) concentration suppressed below 1 ppm. Moreover, increasing the column diameter improved the separation factor up to 3840 while maintaining complete Au(III) recovery, due to the more effective washing out of impurities.

Kozlowski et al. [42] presented β-Cyclodextrin (β-CD) polymers as efficient collectors for Cu(II). β-CD polymers are biocompatible cyclic oligosaccharides that do not induce immune responses and show low toxicity for animals and humans. These polymers achieved 93 % removal of Cu(II) through an ion flotation process from dilute aqueous solutions in the presence of a frother. β-Cyclodextrin forms chelate complexes with metal ions through deprotonated hydroxyl groups, with the stability of these complexes increasing as the pH rises. The molecular weight, polymer linkers, and pH of the solution influenced the collector's performance.

### 2.1.4. *Summary*

Polymers as collectors need greater attention. These examples

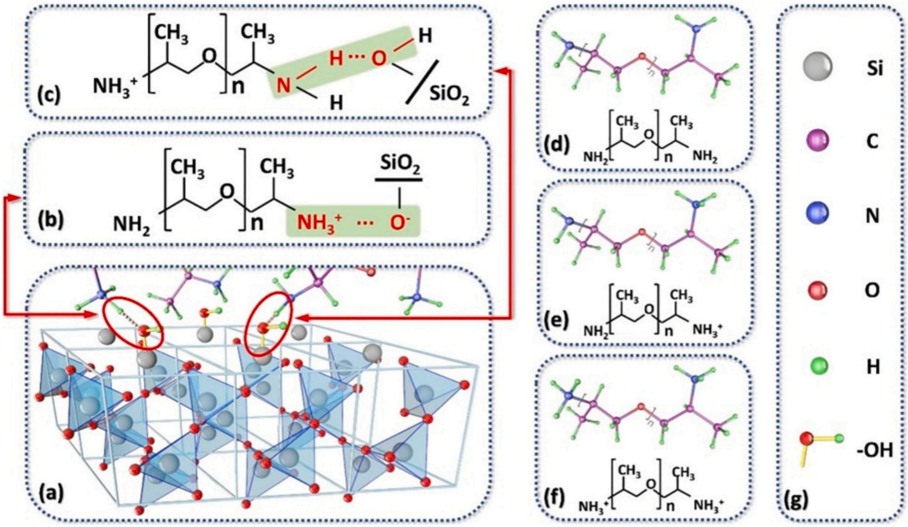

**Fig. 4.** (a)-(c) PEA adsorption model diagram. (d)-(f) Different forms of PEA in water. (g) Schematic diagram of different components [34]. Copyright 2021 Elsevier Ltd.

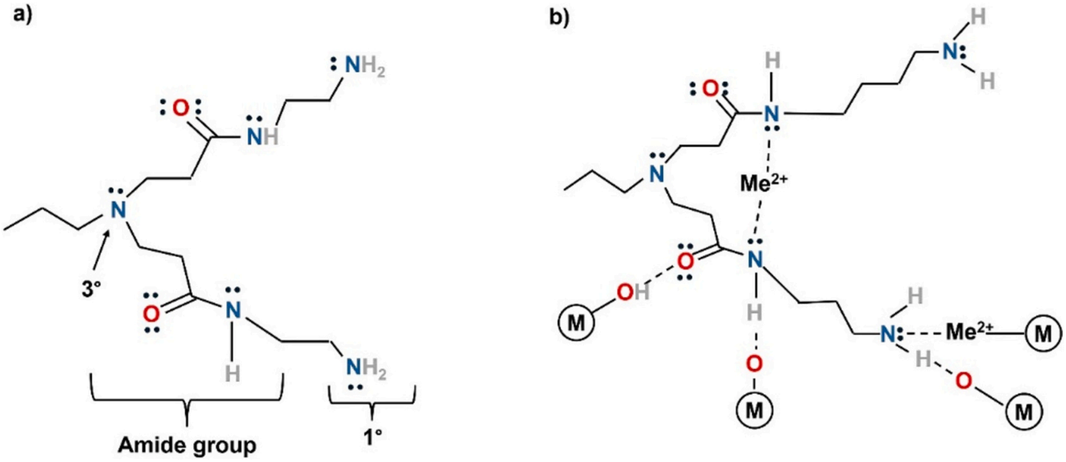

**Fig. 5.** PAMAM dendrimer arms a) and PAMAM-magnetite (M) interaction b). Based on [37].

highlight their potential efficiency. Notably, these polymers are not only greener alternatives but also achieve good results with both primary resources and secondary ones, such as photovoltaic industry waste and leaching solutions from zinc refinery residues. Specifically, β-Cyclodextrin (β-CD), a biocompatible cyclic oligosaccharide, is a promising alternative for copper ion separation.

The primary mechanisms employed by these polymers are electrostatic attraction and affinity for metal ions, with potential coordination and chelation. Maintaining process selectivity with cationic polymers under alkaline conditions can be challenging; however, with a solid understanding of the material and optimization of other factors, is achievable. Good example is PEA. Selectivity in quartz-feldspar flotation with PEA as polymeric collector was achieved by targeting specific particle size range of 150–270 μm, where quartz remains highly floatable while feldspar floatability rapidly decreases. Another factor that enhances selectivity is the presence of positive ions on the feldspar surface, which generates electrostatic repulsion with PEA, preventing adsorption.

Other polymers such as PAMAM, rely not only on electrostatic forces but also on coordination with metal ions through amine and amide groups. PONPE, like β-Cyclodextrin, also demonstrates an affinity for certain metal ions, coordinating or chelating them to form complexes that enhance selectivity.

### 2.2. *Nanoparticles (NPs)*

Yang et al. [43] presented a novel concept in the field of flotation collectors. Their idea was based on utilizing polystyrene hydrophobic nanoparticles (NPs) capable of adsorbing onto significantly larger, hydrophilic mineral particle surfaces to enhance attachment to air bubbles in flotation. Nanoparticles flotation collectors are expected to impact two critical stages in the flotation process: the attachment of mineral particles to the air bubble surface following collision, and the prevention of undesirable detachment of these mineral particles from the bubbles. The main conclusion from their work [43] was that less than 10 % coverage of the glass beads can achieve high flotation efficiency. The authors also suggested that smaller and more hydrophobic particles can be the most effective collectors. The maximum pull-off force for a nanoparticle-coated sphere from a bubble can reach 1.9 μN. Additionally, the authors proposed that the area between the glass bead and the air bubble can remain wet, except for the spots where nanoparticles protrude. The presented positive results brought the high attention of scientific community to the nanoparticle collector.

Researchers focused on answering scientific questions about nanoparticles (NPs) and establishing the optimal range of their features. Yang and Pelton [44] showed that the minimum advancing contact angle for NPs collectors to achieve high flotation recovery is in the range of

30–40° (similar to molecular collectors). Yang et al. [45] mentions that for sufficient NPs coverage with high flotation results, a conditioning time of 5 to 30 min is needed. Additionally, it is highlighted that smaller NPs are more efficient due to faster deposition. A certain mass of smaller NPs can cover a much larger area of the mineral surface and reduce the distance that the three-phase contact line has to move over hydrophilic areas. Interestingly, the authors did not find evidence of NPs desorption from glass beads when their diameter is below 79 nm. Moreover, these glass beads can be refloated without any collector. The work presented in [46] showed that harder (less soft) NPs improve flotation recovery, particularly when their glass transition temperature is close to the flotation temperature. However, softer NPs, due to their greater contact area and better adhesion to mineral particles, lead to higher flotation efficiency. This was also proven in paper [47], where soft-shelled particles exhibited stronger adhesion to glass, thereby improving flotation recovery. Additionally, Janus NPs with soft poly(n-butyl methacrylate) lobes were presented as effective collectors. Dong et al. [48] highlighted the problem of NPs abrasion during collisions among glass beads. Abraded NPs create large aggregates that limit their collecting behavior and leave soft polymer footprints on the glass beads [49]. Another challenge for NPs collector was described in [50]. High ionic strength of the flotation pulp causes NPs to coagulate, requiring higher NPs dosages for the flotation process. To prevent this phenomenon, a balance between NPs charge (to prevent coagulation) and hydrophobicity (to induce flotation) must be found. Abarca et al. [51] lists the advancing water contact angle and the critical coagulation concentration (CCC) values as the main factors in evaluating the usefulness of NPs as flotation collectors.

The summary of the performance and characteristics of nanoparticle collectors is presented in following sections and Table 2.

### 2.2.1. Glass beads separation

In studies [43–49], the nanoparticles exhibit a cationic charge from the positively charged cetyltrimethylammonium bromide (CTAB) and the polymerization initiator 2,2′-azobis(2-methylpropionamidine) dihydrochloride (V50) cationic amidine group. However, extra monomers were added to enhance the cationic character of the nanoparticles (e.g., MAPTAC [43–45], VBTMAC [44]), or control the level of hydrophobicity (HEMA [44]) or adjust the particle softness and shape (N-butyl methacrylate [47,49], methyl methacrylate [47,49], butyl acrylate [46]). The second common finding across all research studies [43–49] is that the recovery rate of negatively charged glass beads by cationic NPs reached 90 % or higher.

### 2.2.2. Pentlandite separation

After glass bead flotation further research involved nickel-bearing minerals, particularly pentlandite ($Ni_{4.5}Fe_{4.5}S_8$) [46,50,51]. It's worth noting that the surface of pentlandite carries a negative charge within the pH range of 2–12 [52]. As mentioned earlier, the cationic character of NPs arises from the presence of surface amidine groups from the cationic polymerization initiator V50. In research [46] collector adsorption capabilities were increased by conducting pretreatment of the nanoparticles with poly(allylamine hydrochloride) (PAAm) and polyvinylamine (PVAm) prior to pentlandite and ultramafic low-grade nickel ore flotation. Both polymers are cationic and possess amine groups capable of coordinating with nickel ions. In both flotation processes, better results were observed with nanoparticles pre-adsorbed with PVAm (referred to as NP5). In the pentlandite flotation, recovery reached 75 %, while in the case of nickel ore, the cumulative nickel recovery and cumulative grade reached 38 % and 4.2 %, respectively.

Research [50] also focused on nickel separation using polystyrene cationic NPs. Two main groups of NPs were tested. Both were composed of styrene and 1-vinylimidazole (VI), but one group included additional monomers such as MAPTAC. The incorporation of VI was aimed at introducing imidazole groups that can bind nickel ions (Fig. 6). The authors proposed that the deposition of these nanoparticles onto pentlandite is facilitated by chemisorption. Flotation tests were conducted using an artificial mixture of washed pentlandite and ultramafic Mg/Si slime tails with the nanoparticle collector St-VI-MAPTAC-158, and for comparison with potassium amyl xanthate (PAX). The dosage of the nanoparticles was 6.7 times higher than that of PAX. However, better flotation performance was achieved with NPs, resulting in a cumulative nickel recovery of approximately 87 % and a cumulative nickel grade of around 17 %, compared to PAX with a cumulative nickel recovery and grade around 75 % and 14 %, respectively. Results from the flotation tests on nickel ore demonstrated a better cumulative nickel grade of up to 3 % achieved by St-VI-52 NPs compared to PAX (approximately 8 % vs. approximately 5 %), but a lower cumulative nickel recovery by 10 % in favor of PAX (64 % vs. 73.5 %). Despite the satisfactory results achieved by the NPs collector, the dosage required is 15.4 times higher than that of PAX.

In article [51], authors tested a large library of NPs with the addition of poly(ethylene glycol) methyl ether methacrylate (PEGMA) and 1-vinylimidazole (VI). Unfortunately, the addition of PEGMA made the nanoparticles too hydrophilic, thereby reducing their flotation performance. For ultramafic nickel ore flotation, nanoparticles designated as PSVI-52 (composed of styrene and VI) were used. They were able to duplicate similar results to research [50] with a high cumulative nickel grade of around 9 %, and a cumulative nickel recovery of approximately 65 %. However, the NPs dosage was also as high as in research [50].

### 2.2.3. Coal separation

An et al. [53] discussed and investigated cationic hydrophobic polystyrene nanoparticles as a collector in flotation of coal fines with an ash content of about 24 %. The authors highlighted slime coating as a significant difficulty in fine coal flotation. Clay particles from the slime create a coating on negatively charged coal through electrostatic attraction with the positively charged edges of slime particles. This process renders coal hydrophilic and increases reagent utilization. Hydrophobic polystyrene NPs offer a potential solution to this issue, as they tend to attach to coal surfaces primarily driven by hydrophobic interactions. Coal exhibits stronger hydrophobicity compared to fine clays. Additionally, electrostatic forces exist between negatively charged coal particles and positively charged NPs.

The flotation performance showed that a higher combustible matter recovery of 86 % was achieved with NPs compared to diesel oil, which achieved 81 %. However, the ash content was lower with diesel oil as a collector, at around 10 %, which is 1 % less than with NPs. While the utilization of NPs offers advantages, the dosage required is 5 times higher compared to diesel oil. Additionally, a poor selectivity of the nanoparticles towards coal was observed [53].

In studies focusing on low rank coal (LRC) flotation [54–56] cationic polystyrene NPs exhibited superior combustible matter recoveries compared to those achieved with diesel oil as the collector. NPs achieved recoveries between 75 and 78 % with a dosage of 16 kg/t, whereas diesel oil recovery was approximately 45–48 %. The enhanced performance of NPs was attributed to the implementation of tetrahydrofurfuryl functional groups (derived from tetrahydrofurfuryl methacrylate) onto the NPs. These functional groups were capable of forming hydrogen bonds with the coal's oxygenated functional groups, thereby improving flotation efficiency (Fig. 7).

### 2.2.4. Cassiterite separation

In research [57], a cationic polystyrene NPs collector was developed to address the issue of poor flotation efficiency in fine cassiterite. During the emulsion polymerization process, the NPs were incorporated with 2-butenohydroxamic acid. In flotation tests, the NPs demonstrated higher recovery rates for cassiterite (96 %) compared to calcite (18 %) under optimal conditions (pH 10.5 and 450 mg/L MPNs), indicating better selectivity for cassiterite than benzohydroxamic acid (BHA) under the pH 6.5 and with a lower dosage of 100 mg/L. At this dosage, cassiterite recovery reached 62 % and calcite 45 %. The interaction of NPs with

**Table 2**
The nanoparticle collectors' performance and adsorption characteristics (NG-not given).

| Polymers/ monomers used/ collector MW | Other agents used in NPs | Targeted mineral | Adsorption on mineral surface | Separation performance | Conventional performance (comparison) | Contact angle | Electrophoretic mobility ($\times 10^{-8}$ $m^2\,s^{-1}\,V^{-1}$) or Zeta potential | Reference |
|---|---|---|---|---|---|---|---|---|
| Styrene,<br>3-(Methacryloylamino) propyl trimethyl ammonium chloride solution (MAPTAC),<br>Vinylbenzyltrimethyl ammonium chloride (VBTMAC),<br>2-hydroxyethyl methacrylate (HEMA) | Cetyltrimethyl ammonium bromide (CTAB),<br>2,2′-azobis(2-methylpropionamidine) dihydrochloride (V50) | Glass beads (particle size 30–50 μm) | Amidine groups on nanoparticles (NPs) exhibit cationic properties. By adding MAPTAC or VBTMAC, more cationic ammonium groups alongside the amidine ones are introduced. Hydroxyethyl groups from HEMA boost the hydrophilicity of NP surfaces. | 0.12 mL of 1 % UNIFROTH 250C<br>1.0 mL/2 g<br>St-01-46:<br>Glass beads recovery $\sim$100 %<br>0.12 mL of 1 % UNIFROTH 250C<br>St-MAPTAC-02-120:<br>Glass beads recovery $\sim$50 %<br>St-01-46:<br>Glass beads recovery $\sim$90 % | NG | St-01-46:<br>$\theta_a = 93^\circ$, $\theta_r = 87^\circ$, $\theta_s = 91^\circ$<br>St-MAPTAC-02-120:<br>$\theta_a = 86^\circ$; $\theta_r = 85^\circ$<br>St-01-46:<br>$\theta_a = 93^\circ$; $\theta_r = 91^\circ$ | Electrophoretic mobility:<br>St-01-46:<br>$\sim$ 2<br>St-MAPTAC-02-120:<br>$\sim$ 3<br>St-01-46:<br>$\sim$ 2 | [43]<br>[44] |
| Styrene,<br>MAPTAC,<br>Fluorescein dimethacrylate | CTAB,<br>V50,<br>Ammonium Persulfate (APS) | Glass beads (particle size 30–50 μm) | Electrostatic interaction. Cationic nanoparticles spontaneously adsorbed onto the negatively charged beads. | 0.12 mL of 1 % UNIFROTH 250C<br>1 mL/2 g<br>NP46:<br>Glass beads recovery $\sim$90 %<br>NP79:<br>Glass beads recovery $\sim$80 % | NG | NP46:<br>$\theta_{npr} = 93^\circ$<br>NP79:<br>$\theta_{npr} = 75^\circ$ | Electrophoretic mobility:<br>NP46:<br>$\sim$2<br>NP79:<br>$\sim$ 2 | [45] |
| Styrene,<br>N-butyl methacrylate,<br>Methyl methacrylate | CTAB,<br>V50,<br>Potassium bromide | Glass beads (particle size with a mean diameter of 43 ± 11 μm) | Cationic polystyrene-core-poly(n-butyl methacrylate)-shell (PS–PB) nanoparticles. | 0.125 mL of 1 % UNIFROTH 250C<br>20 mg/2 g of PS–PB3 core–shell NPs:<br>Glass bead recovery $\sim$91 %<br>5 mg/2 g of PS/PB Janus NPs:<br>Glass bead recovery $\sim$99 % | NG | PS–PB3 core-shell:<br>$\theta_{npr} = 60^\circ$<br>PS/PB Janus:<br>$\theta_{npr} = 84^\circ$ | Electrophoretic mobility:<br>PS–PB3 core-shell:<br>$\sim$ 4<br>PS/PB Janus:<br>$\sim$ 2 | [47] |
| Styrene | CTAB,<br>V50 | Glass beads (particle size with a mean diameter of 43 ± 11 μm) | Electrostatic interaction. Cationic amidine groups on the polystyrene surface. | 0.125 mL UniFroth (1 wt%)<br>5 mg/2 g of PS63 NPs:<br>Glass beads recovery $\sim$90 %<br>2 mg/2 g of PS63 NPs:<br>Glass beads recovery $\sim$60 % | NG | PS63:<br>$\theta_{npr} = 76^\circ$ | Electrophoretic mobility:<br>PS63:<br>$\sim$2 | [48] |
| Styrene,<br>N-butyl methacrylate,<br>Methyl methacrylate | CTAB,<br>V50,<br>Potassium bromide,<br>Dowex MB mixed bed ion-exchange resin | Glass beads (particle size with a mean diameter of 43 ± 11 μm) | Cationic polystyrene-core-poly(n-butyl methacrylate)-shell (PS–PB) nanoparticles. | 0.125 mL UniFroth (1 wt%)<br>5 mg/2 g<br>PS/PB-92 Janus:<br>Glass beads recovery $\sim$99 %<br>PS/PB-315 Janus: | NG | PS/PB-92 Janus:<br>$\theta_{npr} = 84^\circ$<br>PS/PB-315 Janus:<br>$\theta_{npr} = 65^\circ$<br>PS-PB-356 | Electrophoretic mobility:<br>PS/PB-92 Janus:<br>$\sim$ 2<br>PS/PB-315 Janus:<br>$\sim$ 5<br>PS-PB-356 core- | [49] |

(*continued on next page*)

**Table 2** (*continued*)

| Polymers/ monomers used/ collector MW | Other agents used in NPs | Targeted mineral | Adsorption on mineral surface | Separation performance | Conventional performance (comparison) | Contact angle | Electrophoretic mobility (× $10^{-8}$ $m^2$ $s^{-1}$ $V^{-1}$) or Zeta potential | Reference |
|---|---|---|---|---|---|---|---|---|
| | | | | Glass beads recovery ~90 %<br>PS-PB-356 core-shell:<br>Glass beads recovery ~60 % | | core-shell:<br>$\theta_{npr} = 60^\circ$ | shell:<br>~4 | |
| Styrene,<br>Butyl acrylate | V50,<br>Polyvinylamine (PVAm),<br>Poly(allylamine hydrochloride) (PAAm) | Glass beads (particle size 30–50 μm)<br>Purified high grade pentlandite (Pn) with 27 % Ni content (particle size with Sauter mean diameter of 12 μm)<br>Ultramafic low-grade (~ 0.47 %) nickel sulfide ore (particle size <106 μm) | The nanoparticles are positively charged because of the presence of surface amidine groups from the cationic polymerization initiator V50. PVA is a nickel chelating polymer. | 0.12 mL of 1 % UNIFROTH 250C (10 ppm)<br>0.5 mL/2 g of NP5, pH ~6.7:<br>Glass beads recovery ~90 %<br>0.5 mL/ 2 g of NP5, pH ~8.4:<br>Pn recovery ~75 %<br>20 ppm UNIFROTHER 250C (ore)<br>0.8 g/kg of NP5 with PVAm, pH 8.5, (ore):<br>Nickel (Ni) recovery ~38 %<br>Ni grade ~ 4.2 %<br>0.8 g/kg of NP4 with PAAm, pH 8.5, (ore):<br>Ni recovery ~35 %<br>Ni grade ~ 3.2 % | NG | NP5:<br>$\theta sa_r = \sim 96^\circ$<br>$\theta r_r = \sim 41^\circ$<br>NP4:<br>$\theta sa_r = \sim 91^\circ$<br>$\theta r_r = \sim 36^\circ$ | Electrophoretic mobility:<br>NP5; NP4: ~3 | [46] |
| Styrene,<br>MAPTAC,<br>1-vinylimidazole (VI) | CTAB,<br>V50 | Synthetic ore: Purifed high grade pentlandite (Pn) with 27 % Ni content (particle size with mean diameter of 12 μm) and Mg/Si slime tails.<br>Complex ultramafic low-grade nickel sulfide ore (particle size <106 μm). | Imidazole groups bind nickel ions, authors propose that the VI nanoparticle deposition onto pentlandite is facilitated by chemisorption. | 0.12 mL of 1 % UNIFROTH 250C<br>11.1 mg/g of St-VI-MAPTAC-158 (synthetic ore):<br>Ni recovery ~87 %<br>Ni grade ~ 17 %<br>20 ppm UNIFROTH 250C<br>1000 g/t of St-VI-52, pH 8.6 (ore):<br>Ni recovery ~64 %<br>Ni grade ~ 8 % | 5 mg/3 g of Potassium amyl xanthate (PAX) (synthetic ore):<br>Ni recovery ~75 %<br>Ni grade ~ 14 %<br>65 g/t PAX (ore):<br>Ni recovery ~74 %<br>Ni grade ~ 5 % | St-VI-MAPTAC-158:<br>$\theta = 36^\circ$<br>St-VI-52:<br>$\theta = 44^\circ$ | Electrophoretic mobility:<br>St-VI-MAPTAC-158:<br>~ 3<br>St-VI-52:<br>~ 2 | [50] |
| Styrene,<br>Poly(ethylene glycol) methyl ether methacrylate (PEGMA),<br>VI | V50 | Glass beads (particle size 30–150 μm).<br>Ultramafic nickel ore (particle size <106 μm). | Electrostatic interaction.<br>Imidazole groups affinity to nickel ions. | 0.12 mL of 1 % Unifroth 250C<br>100 mg/2 g of PS-62 NPs, pH ~ 9–10:<br>Glass beads recovery ~81 %<br>10 ppm of frother (Unifroth 250C)<br>1000 g/t of PSVI-52, | NG | PS-62:<br>$\theta = 71^\circ$<br>PSVI-52:<br>$\theta = 61^\circ$ | Electrophoretic mobility:<br>PS-62:<br>~3<br>PSVI-52:<br>~ 3 | [51] |

(*continued on next page*)

**Table 2** (*continued*)

| Polymers/ monomers used/ collector MW | Other agents used in NPs | Targeted mineral | Adsorption on mineral surface | Separation performance | Conventional performance (comparison) | Contact angle | Electrophoretic mobility (× $10^{-8}$ $m^2$ $s^{-1}$ $V^{-1}$) or Zeta potential | Reference |
|---|---|---|---|---|---|---|---|---|
| | | | | pH 10<br>Ni recovery ∼65 %<br>Ni grade ∼ 9 % | | | | |
| Styrene | CTAB,<br>V50 | Anthracite coal ore (particle size <0.5 mm). | Hydrophobic NPs tend to attach to coal surfaces, driven primarily by hydrophobic interactions. Coal exhibits stronger hydrophobicity compared to fine clays. Electrostatic forces exist between negatively charged coal particles and positively charged NPs. | Frother: 2-octanol 100 g/t<br>2.5 kg/t of NPs, pH 8:<br>Combustible matter recovery ∼86 %<br>Ash content ∼11 % | Frother: 2-octanol 100 g/t<br>0.5 kg/t Diesel oil (DO), pH 8:<br>Combustible matter recovery ∼81 %<br>Ash content ∼10 % | NP collector:<br>θ = 75°<br>DO:<br>θ = 70° | Zeta potential (at pH 8):<br>NP: 28 mV | [53] |
| Styrene,<br>Tetrahydrofurfuryl Methacrylate (THFMA) | CTAB,<br>V50,<br>Divinylbenzene (DVB) | Low-rank coal (LRC) – gravity concentrated sample from mine (90 % of particles size <74 μm). | Adosrption of NPs collector may be due to both hydrophobic bonding (tetrahydrofurfuryl functional group) and electrostatic attraction (positive CTAB charge) with negatively charged coal surface. | Frother: 2-octanol 100 g/t<br>16 kg/t St-100-0.74 NPs, pH 8:<br>LRC recovery ∼75 %<br>16 kg/t St-100-1.48 NPs, pH 8:<br>LRC recovery ∼68 % | Frother: 2-octanol 100 g/t<br>16 kg/t DO:<br>LRC recovery ∼45 % | St-100-1.48:<br>θ = 110°<br>DO:<br>θ = 58° | Zeta potential (at pH 8):<br>St-100-0.74<br>49 mV<br>St-100-1.48<br>50 mV | [54] |
| Styrene,<br>2-Hydroxyethyl Methacrylate (HEMA)/ THFMA | DVB,<br>Sodium dodecyl sulfate (SDS)/ CTAB,<br>V50 | Low-rank coal (LRC) – concentrate product of LRC after gravity separation from processing plant (particle size <74 μm) | The cationic NPs are positively charged, suggesting an electrostatic driving force. Driven by hydrophobic force and electrostatic attraction, the cationic nanoparticles are easier to adsorb onto the target coal surface. The hydrogen bonds between TFPNs/ HFPNs and LRC (tetrahydrofurfuryl/ hydroxyl groups). | Frother: 2-octanol 100 g/t<br>4, 8, 12, 16 kg/t of TFPNs:<br>LRC recovery ∼55, ∼65, ∼75, ∼78 %,<br>4, 8, 12, 16 kg/t of HFPNs:<br>LRC recovery ∼45–50 % | Frother: 2-octanol 100 g/t<br>4, 8, 12, 16 kg/t of DO:<br>LRC recovery ∼26, ∼35, ∼40, ∼45 % | TFPNs:<br>θ = 87° – 110°<br>HFPNs:<br>θ = 82°<br>DO:<br>θ = 57° | Zeta potential:<br>Cationic TFPNs/ HFPNs ZP varies with CTAB dosage:<br>from 26 mV to 50 mV | [55] |
| Styrene,<br>THFMA | DVB,<br>SDS/ CTAB,<br>Azobisisobutyronitrile (AIBN) | Low-rank coal (LRC) – LRC product after gravity separation from processing plant (particle size <74 μm) | The adsorption of TFPNs occur by forming hydrogen bonds between tetrahydrofurfuryl groups and coal oxygen-containing functional groups. | Frother: 2-octanol 100 g/t<br>4, 8, 12, 16 kg/t of TFPNs:<br>LRC recovery ∼55, ∼65, ∼75, ∼78 %, | Frother: 2-octanol 100 g/t<br>4, 8, 12, 16 kg/t of DO:<br>LRC recovery ∼42, ∼45, ∼46, ∼48 % | TFPNs:<br>θ = 112° | Zeta potential:<br>Cationic TFPNs varies with CTAB dosage:<br>from 25 mV to 50 mV | [56] |
| Styrene | CTAB,<br>V50,<br>2-butenyl hydroxamic acid (2-BHA) | Cassiterite – pure mineral (particle size <10 μm) | Electrostatic interaction with the cationic NPs and negatively charged cassiterite.<br>Hydroxamic acid group on the surface of NPs formed complex with $Sn^{2+}$. | Frother: terpineol 10 mg/L<br>450 mg/L of NPs, pH 10.5 (pure mineral flotation:<br>Cassiterite recovery ∼95 %,<br>Calcite recovery ∼18 % | 100 mg/L of hydroxamic acid (BHA), pH 6.5:<br>Cassiterite recovery ∼62 %,<br>Calcite recovery ∼45 % | NG | Zeta potential (under experimental conditions):<br>NPs:<br>42 mV<br>Cassiterite + NPs:<br>−40 mV<br>Calcite _NPs:<br>∼ 0 mV | [57] |
| Styrene,<br>2-mercapto benzothiazole (MBT) | SDS,<br>APS | Chalcopyrite – pure mineral with Cu grade 33 % (particle size <23 μm) | The adsorption form of NPs onto chalcopyrite surface is chemical absorption. Chemisorptive bonds could be formed between N atom and Cu surface, eventually with S atom. | Flotation only with collector<br>1 mL/2 g of HNP, pH 6:<br>Chalcopyrite recovery ∼96 % | NG | NG | Zeta potential of chalcopyrite with HNPs at pH 6:<br>−5 mV | [58] |

(*continued on next page*)

**Table 2** (*continued*)

| Polymers/ monomers used/ collector MW | Other agents used in NPs | Targeted mineral | Adsorption on mineral surface | Separation performance | Conventional performance (comparison) | Contact angle | Electrophoretic mobility (× $10^{-8}$ $m^2$ $s^{-1}$ $V^{-1}$) or Zeta potential | Reference |
|---|---|---|---|---|---|---|---|---|
| Styrene,<br>VI | CTAB,<br>V50 | Chalcopyrite – high purity mineral (particle size 75–150 μm) | Chalcopyrite recovery with St-CTAB occurs because cationic particles deposit onto the mineral surface via electrostatic and Van der Waals forces. With St-CTAB-VI, the imidazole group additionally facilitates imidazole-copper complex formation, enhancing recovery. | Frother: Aerofroth 10 ppm<br>17.73 mg/g of St-CTAB-VI NPs, at pH 6, 8:<br>Chalcopyrite recovery 98 %, 94 %<br>18.62 mg/g at pH 6; 24.91 mg/g at pH 8<br>St-CTAB NPs:<br>Chalcopyrite recovery 98 %, 87 %, | Frother Aerofroth 10 ppm<br>8.4 mg/g of PAX, at pH 6, 8:<br>Chalcopyrite recovery ~95 %, 91 % | NG | Electrophoretic mobility:<br>St-CTAB-VI at pH 6; 8: ~3<br>St-CTAB at pH 6; 8: ~5<br>Zeta potential:<br>St-CTAB-VI at pH 6; 8: 43; 39 mV<br>St-CTAB at pH 6; 8: 62; 60 mV | [59] |
| Styrene,<br>Butyl acrylate | 2,2-Azobis (2-methylpropyl) dihydrochloride (AIBA) | Chalcopyrite – pure mineral sample (particle size <38 μm) in presence of serpentine (pure mineral with particle size <10 μm) | The chalcopyrite surface carries a negative charge, while the St-Ba surface is positively charged, leading to electrostatic attraction between them. Both surfaces are hydrophobic, resulting in attractive forces between the particles. | Frother MIBC<br>1.76 g/L of St-Ba NPs, pH 8, 10 (artificial mixture of chalcopyrite and serpentine):<br>Chalcopyrite recovery ~80 %,~ 82 % | Frother MIBC<br>$1 \times 10^{-4}$ mol/L of Sodium Butyl Xanthate (SBX), pH 8, 10 (artificial mixture of chalcopyrite and serpentine):<br>Chalcopyrite recovery ~60 %, ~ 42 % | Chalcopyrite with St-Ba:<br>θ > 70° | NG | [60] |
| Chitin | Hexanal,<br>Octanal,<br>Decanal | Malachite – mineral sample (particle size 20–150 μm) | Chitin nanocrystals positive surface charges are expected to promote electrostatic attraction towards the malachite surface. | Hallimond tube, 3 mg/g of DA-Dec, at pH 3:<br>3 days DA-Dec: Malachite recovery ~18 %<br>7 days DA-Dec: Malachite recovery ~28 %<br>3 h at 80° DA-Dec: Malachite recovery ~34 % | Hallimond tube, 3 mg/ g of DDA, at pH 3:<br>Malachite recovery ~31 % | 3 days:<br>DA θ = 44°<br>DA-Hex θ = 60°<br>DA-Oct θ = 71°<br>DA-Dec θ = 75°<br>7 days:<br>DA-Hex θ = 66°<br>DA-Oct θ = 72°<br>DA-Dec θ = 73°<br>3 h at 80°:<br>DA-Dec θ = 84° | Zeta potential<br>Malachite ~ −21 mV<br>DA-ChNC ~27 mV<br>DA-Dec at pH 3:<br>3 h ~ 17 mV<br>3 days ~18 mV<br>7 days ~14 mV<br>3 h at 80° ~18 mV | [61] |
| Lignin<br>(birch lignin MW = 4200 Da;<br>Spruce lignin MW = 4600 Da) | none | Metals: Cu, Ni, Co, Pb, Zn<br>Cu—Ni Ore A:<br>0.5 % Cu, 0.3 % Zn, 0.3 % Ni, 12.3 % Fe, and 6.8 % S<br>Cu—Ni Ore B:<br>0.4 % Cu, 0.4 % Zn, 0.3 % Ni, 6.8 % Fe, 3.1 % S<br>Zn-Pb-Cu ore: | NG | **Ore A**, I stage pH 10.5, II 9–10 (lime),<br>Birch lignin microparticles (BM):<br>Cu recovery - 70 %, grade 8.6 %<br>Birch lignin nanoparticles (BN):<br>Cu recovery - 77 %, grade 7.9 %<br>Fe recovery in all lignin trials below | **Ore A** I stage pH 10.5, II 9–10 (lime),<br>Isobutyl Xanthate (IBX):<br>Cu recovery 92 %, grade 9.2 %<br>Fe recovery 91 %<br>With activator Aerophine®:<br>Cu recovery 96 %, grade 16.6 %<br>Ni recovery 94 % | NG | Zeta potential at pH 9:<br>BN: −38 mV<br>BM: −21 mV<br>Spruce Nanoparticles (SN): −52 mV<br>Spruce Microparticles (SM):- 56 mV<br>Zeta potential at pH 10: | [62]<br>[63] |

(*continued on next page*)

**Table 2** (*continued*)

| Polymers/ monomers used/ collector MW | Other agents used in NPs | Targeted mineral | Adsorption on mineral surface | Separation performance | Conventional performance (comparison) | Contact angle | Electrophoretic mobility (× $10^{-8}$ $m^2$ $s^{-1}$ $V^{-1}$) or Zeta potential | Reference |
|---|---|---|---|---|---|---|---|---|
| | | 0.4 % Cu, 7.1 % Zn, 1.0 % Pb | | 15 %.<br>For BM:<br>pH 10.5 (NaOH):<br>Cu recovery - 82 %, grade 9.6 %<br>With activator Aerophine®:<br>Cu recovery 97 %, grade 9.9 %<br>Ni recovery 92 %, grade 2.5 %<br>Fe recovery below 82 %<br>**Ore B** I stage pH 10.5, II 9–10 (lime), BM with depressant CMC:<br>Cu recovery - 74 %, grade 7.9 %<br>Ni recovery 68 %, grade 2.4 %,<br>Co recovery - 38 %, grade 0.1 %<br>Fe recovery 58 %<br>**The Zn-Pb-Cu ore** I stage pH 10.5, II 11.5 (lime) for BL:<br>Cu recovery - 67 %, grade 1.8 %<br>Pb recovery - 73 %, grade 6.2 %,<br>Zn recovery - 47 %, grade 9,5 % | Fe recovery 91 %<br>**Ore B** I stage pH 10.5, II 9–10 (lime), Sodium Isopropyl Xanthate (SIPX):<br>Cu recovery 96 %, grade 13.5 %<br>Ni recovery 90 %, grade 3.5 %<br>Co recovery 80 %, grade 0.3 %<br>Fe recovery 58 %, grade 44.9 %<br>**The Zn-Pb-Cu ore** I stage pH 10.5, II 11.5 (lime), SIPX And PAX:<br>Cu recovery - 84 %, grade 9.1 %<br>Pb recovery - 70 %, grade 20.6 %<br>Zn recovery - 96 %, grade 44.7 % | | BN: −42 mV<br>BM: −22 mV<br>Spruce Nanoparticles (SN): −47 mV<br>Spruce Microparticles (SM): −44 mV | |
| Styrene,<br>Butyl acrylate | V50 | Pyrite – pure mineral sample (particle size 34–74 μm) in presence of lizardite (pure mineral with particle size <10 μm) | Electrostatic attraction between negatively charged pyrite NPs cationic $NH^{3+}$ groups. | Frother MIBC (1 × $10^{-4}$ M)<br>600 mg/L of PS-PBNH NPs, pH 8 (pyrite and lizardite slime mixture):<br>Pyrite recovery >90 % | 50 mg/L of Potassium Butyl xanthate (PBX) pH 8 (pyrite and lizardite slime mixture):<br>Pyrite recovery ~38 % | NG | Zeta potential:<br>PS-PBNH + Pyrite at pH 8:<br>15 mV | [64] |
| Styrene,<br>Butyl acrylate | CTAB,<br>APS,<br>PBX | Pyrite from high-sulfur bauxite samples. | The interaction of NPs with pyrite was mainly surface physical absorption, chemical reaction, and electrostatic interaction. | 900 g/t (Rougher), 300 g/t (Cleaner) of St:BA:PBX NPs, pH 9:<br>Aluminum concentrate yield ~86 %<br>sulfur content ~0.36 % | 800 g/t (Rougher), 300 g/t (Cleaner I), 100 g/t (Cleaner II) of commonly used desulfurization collector, pH 9:<br>Aluminum concentrate yield ~86 %<br>sulfur content ~0.56 % | Pyrite with St: BA:PBX:<br>θ = 113° | Zeta potential:<br>Pyrite + St:BA:PBX NPs, pH 9:<br>−15 mV<br>Pyrite: −21 mV | [65] |

(*continued on next page*)

**Table 2** (*continued*)

| Polymers/ monomers used/ collector MW | Other agents used in NPs | Targeted mineral | Adsorption on mineral surface | Separation performance | Conventional performance (comparison) | Contact angle | Electrophoretic mobility ($\times 10^{-8}$ $m^2 s^{-1} V^{-1}$) or Zeta potential | Reference |
|---|---|---|---|---|---|---|---|---|
| Lignin | SDS/ CTAB,<br>APS,<br>PBX/PAX | Pyrite from high-sulfur bauxite samples (particle size <400 mesh ~ < 38 μm). | NPs interaction with pyrite surface, which was contributed to physico-chemical adsorption and electrostatic attraction. | 900 g/t (Rougher), 300 g/t (Cleaner) of Lignin:SDS:PBX NPs, pH 9:<br>Aluminum concentrate yield ~87.57 %<br>sulfur content ~0.38 % | 800 g/t (Rougher), 300 g/t (Cleaner I), 100 g/t (Cleaner II) of commonly used desulfurization collector, pH 9:<br>Aluminum concentrate yield ~86 %<br>sulfur content ~0.56 % | NG | Zeta potential:<br>Lignin:SDS:PBX NPs, pH 9:<br>−25 mV<br>Pyrite: −21 mV | [66] |

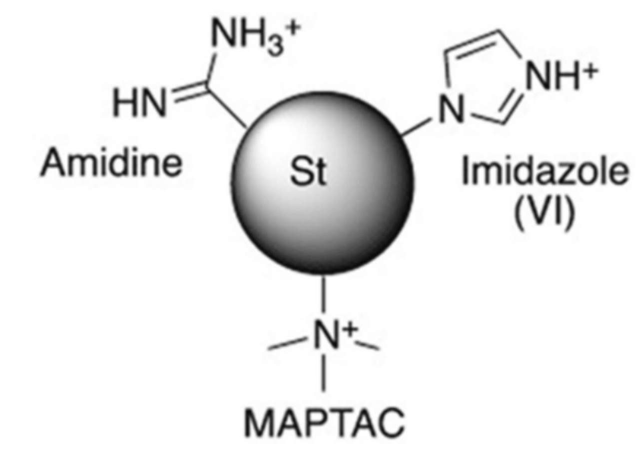

**Fig. 6.** The structural components of the nanoparticle flotation collectors [51]. Copyright 2015 Elsevier Inc.

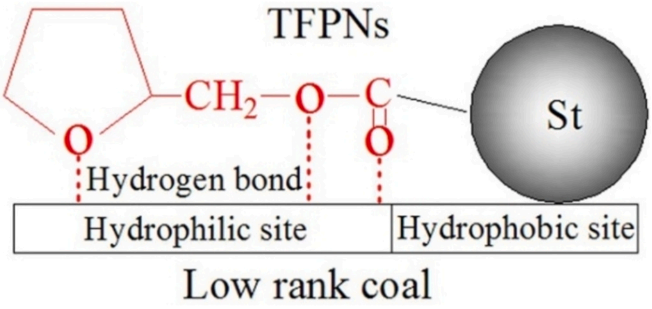

**Fig. 7.** Interaction mechanism of the TFPNs on the low rank coal surface [54]. CC BY license.

cassiterite surfaces may be attributed to the more negative surface potential of cassiterite than calcite and its stronger electrostatic interaction with the cationic NPs. Additionally, the hydroxamic acid group on the surface of NPs formed a more stable complex with $Sn^{2+}$ than with $Ca^{2+}$. These results highlight the selective adsorption of NPs on cassiterite over calcite and their superior performance compared to BHA in the separation of both minerals.

### 2.2.5. *Chalcopyrite separation*

Flotation, as a separation process, exhibits decreased efficiency in separating fine and ultra-fine particles. Fine disseminated minerals require further comminution, even below 30 μm, which was a motivation behind research [58]. In this study, the authors investigated hydrophobic polystyrene NPs with thiazole groups as a collector in microfine chalcopyrite flotation. The selectivity of the NPs collector is attributed to strong chemisorption on chalcopyrite surfaces. Chemisorptive bonds could form between nitrogen and sulfur atoms from the thiazole group and copper ions on the chalcopyrite surface. Chalcopyrite recovery with NPs reached 95 % at pH 6 with a NPs dosage of 0.5 mL/g.

Murga et al. [59] investigated another method for chalcopyrite separation in their research. They prepared two types of polystyrene-based NPs, both containing styrene and CTAB, with one additionally including a VI monomer, named St-CTAB and St-CTAB-VI, respectively. Chalcopyrite recovery with St-CTAB occurred as cationic particles deposited onto the mineral surface through electrostatic and van der Waals forces. With St-CTAB-VI, the imidazole group further facilitated imidazole-copper complex formation, enhancing recovery. NPs collectors achieved the best results at pH 6, with chalcopyrite recovery reaching 98 % for St-CTAB-VI (at a dosage of 17.73 mg/g) and for St-

CTAB (at a dosage of 18.62 mg/g). In comparison, recovery presented by PAX at the same pH and dosage of 8.4 mg/g was approximately 3 % lower.

In the third example of chalcopyrite separation, the role of collector was played by cationic polystyrene-butyl acrylate nanoparticles (St-Ba NPs) [60]. The collection of chalcopyrite was conducted in the presence of serpentine to mimic ore conditions. With St-Ba NPs at a concentration of 1.76 g/L and pH 10, chalcopyrite recovery exceeded 80 %, whereas recovery with sodium butyl xanthate (SBX) (at a dosage of $1 \times 10^{-4}$ mol/L) was only 42 %. Electrostatic attractions occur between the negatively charged chalcopyrite surface and the positively charged St-Ba surface. Both surfaces being hydrophobic, resulted in attractive forces between the particles. It is worth mentioning that the authors believe that the presence of serpentine hinders the floatability of chalcopyrite due to the slime-coating of serpentine fines on the chalcopyrite surface (Fig. 8a). This prevents contact of air bubbles with the SBX adsorbed layer. Meanwhile, the size of the St-Ba nanoparticles adsorbed on the mineral surface helps to attach to air bubbles even in the presence of the slime coating (Fig. 8b).

### 2.2.6. *Malachite separation*

In study [61], the authors presented an alternative to fossil-based and environmentally harmful reagents currently dominant in mineral flotation processes. They proposed using chitin nanocrystals (ChNCs) derived from natural chitin polymer, which have amino groups on their surface, as a greener option for collecting various minerals. The chitin nanocrystals were functionalized with aldehyde structures to increase their hydrophobicity. Contact angle measurements showed the values from 60° to 84°, depending on the type of aldehyde, the duration of the functionalization process, and the temperature. The flotation performance of functionalized N-alkylated chitin nanocrystals was based on electrostatic attraction between the positively charged surface of the nanocrystals and negatively charged malachite (Fig. 9). N-alkylated ChNCs functionalized with decanal showed a slightly better recovery rate of about 34 %, compared to the conventional collector dodecyl amine (DDA), with the recovery of 31 %.

### 2.2.7. *Polymetallic ore separation*

The aim of the study [62] was to investigate novel lignin nanoparticles and microparticles as an ecofriendly collectors for Cu, Ni, and Zn recovery from polymetallic ores. Lignin, a naturally occurring polymer, is widely abundant and characterized by its low cost. Lignin particles had good selectivity towards Cu (chalcopyrite) achieving total recoveries of 70–87 % and grade of 8–9 % in rougher flotation tests using lignin collectors in ore A. Birch lignin microparticles (BM) with the activator Aerophine® was slightly better than isobutyl xanthate (IBX) in copper recovery, with nickel recovery also high at 92 % under these conditions. For a Zn-Pb-Cu ore, the selectivity of lignin collectors shifted towards lead, although their performance was lower than xanthates. However, replacing half of the xanthates with lignin collectors improved the total Zn recovery from the Zn-Pb-Cu ore. These positive results demonstrate the potential of lignin as a collector and the possibility of replacing toxic conventional reagents with environmentally friendly alternatives.

The characterization of lignin particles was studied in [63]. Gel permeation chromatography (GPC) revealed the presence of aliphatic hydroxyl groups (OH), carboxylic (COOH), and phenolic content. At pH levels higher than 4, all examined particles exhibited a zeta (ζ) potential below −20 mV. Generally, as the pH value increased, the ζ potential decreased. Due to the lower ζ potential values at higher pH, lignin particles remained sufficiently stable in dispersion. Organosolv lignin particles showed rigid attachment to chalcopyrite and pyrite. However, the nature of this attachment needs to be further studied to be fully explained.

### 2.2.8. *Pyrite separation*

The application of cationic polystyrene NPs has been explored in pyrite separation, as discussed in research [64]. The utilization of these NPs effectively countered the negative influence of lizardite slime coating in the flotation process. The cationic character of the polystyrene-*co*-poly(n-butylacrylate) NPs (PS-PBNH) was derived from the polymerization initiator V50, enabling electrostatic attraction between the negatively charged pyrite and the $NH_3^+$ groups of NPs. Pyrite recovery achieved with this collector reached 90 %, even in the presence of lizardite in the slurry. In contrast, potassium butyl xanthate (PBX) at the same pH (pH = 8) yielded much lower results, with pyrite recovery around 38 %. Despite the significantly superior performance of the NPs compared to the conventional collector, their dosage was 12 times higher. The success of the NPs as the collector may be attributed to their ability to change the charge of the pyrite surface to positive, potentially causing electrostatic repulsion of the positively charged lizardite particles as well.

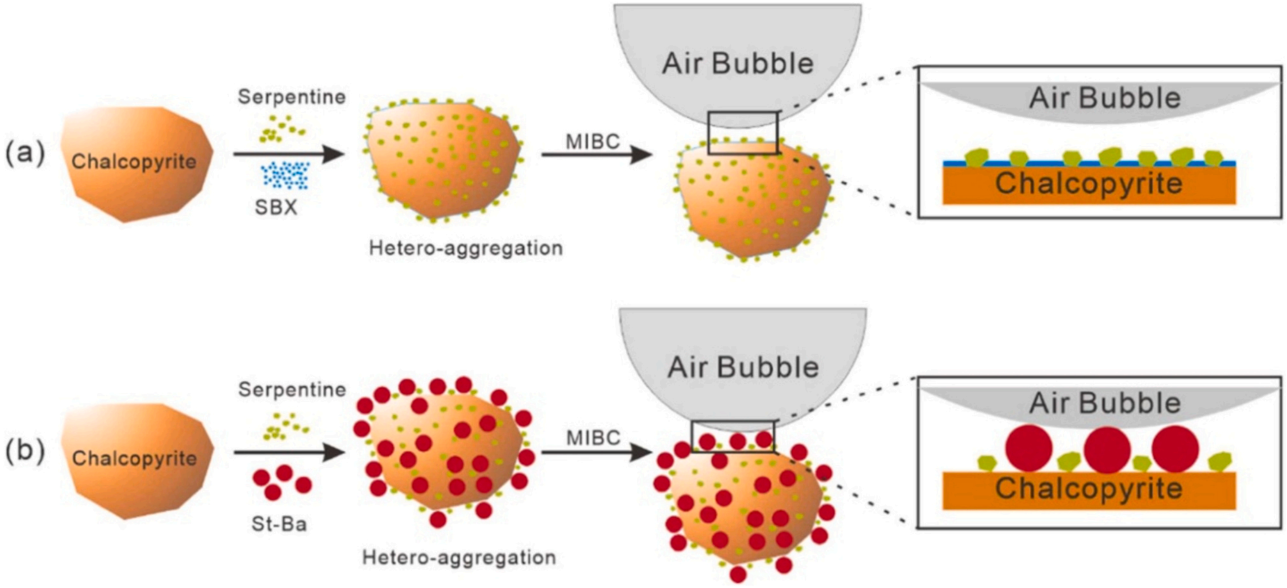

**Fig. 8.** A schematic view on the mechanism of the enhanced floatability of chalcopyrite by St-Ba nanospheres [60]. Copyright 2022 Elsevier B.V.

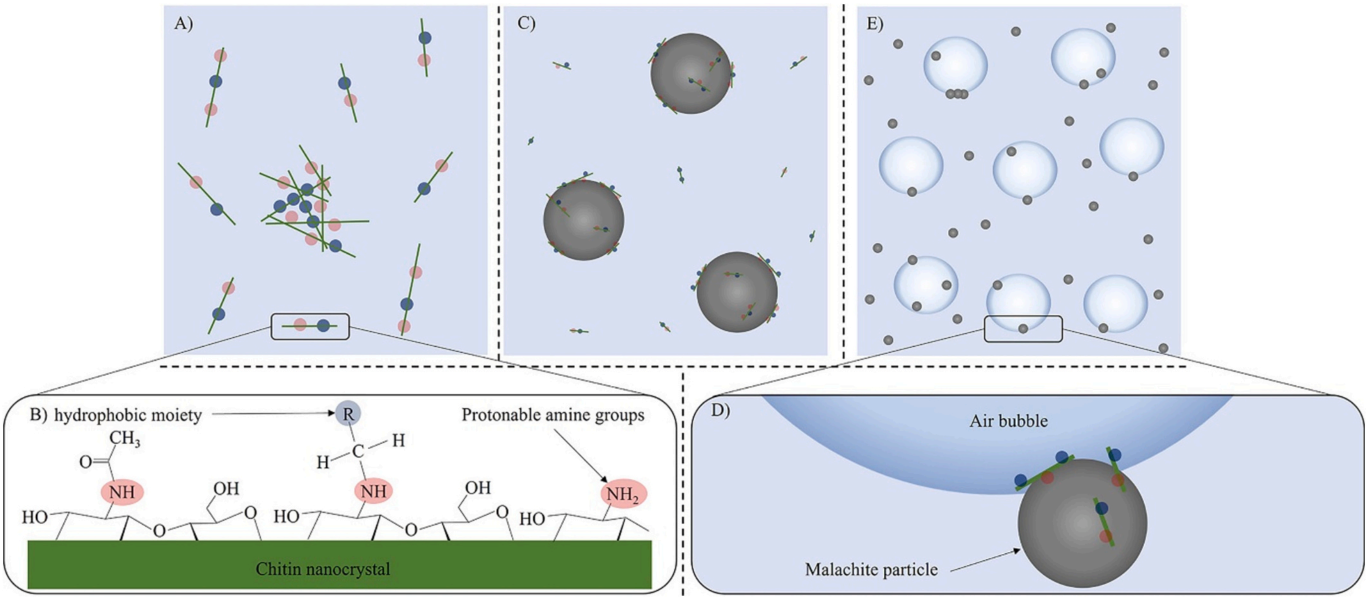

**Fig. 9.** Behavior of functionalized ChNCs during the flotation process [61]. CC-BY 4.0 license.

Cheng et al. [65,66] investigated two types of nanoparticle collectors for the desulfurization of fine high-sulfur bauxite via reverse flotation. One type consisted of styrene (St) and butyl acrylate (BA) as host monomers [65], while the other utilized lignin [66]. The preparation of NPs involved reagents such as CTAB/SDS, APS, and PBX/PAX. In both cases, the interaction of NPs with the pyrite surface contributed to physico-chemical adsorption and electrostatic attraction. Interestingly, the utilization of both NPs collectors enabled a reduction in the number of flowsheet steps from “one roughing - two cleaning - three scavenging” to “one roughing - one cleaning - two scavenging”. The results obtained with the St-BA collector showed an aluminum concentrate with a yield of 86 % and a sulfur content of 0.36 %, while the lignin collector yielded an aluminum concentrate with a yield of 88 % and a sulfur content of 0.36 %. Both collectors achieved lower sulfur content than the traditional collector, with the lignin nanoparticle collector yielding a better aluminum concentrate yield by approximately 2 %.

### *2.2.9. Summary*

Creating NPs for specific mineral beneficiation is a complex task that requires careful consideration of various factors and their interactions. A common strategy involves using a polymeric core such as polystyrene, butyl/methyl acrylate/methacrylate, lignin, or chitin, and functionalizing them with specific chemical reagents. These reagents provide NPs with functional groups that target desired minerals. Mixed forces derived from these functional groups promote NPs adsorption, with some forces dominating. For example, electrostatic attraction is significant with silica or malachite, hydrogen bonding supported by hydrophobic interactions is effective with coal, and coordination/complexation of ions occurs with minerals like pentlandite, cassiterite, chalcopyrite, or pyrite. Functional groups containing nitrogen or sulfur atoms are primarily involved in coordination or complexation.

NPs should be tailored for each process, considering the ion strength of the pulp and affinity towards specific ions on the mineral surfaces. Moreover, the structure of NPs needs to balance their charge and hydrophobicity. The creator must consider the number of hydrophobic functional groups to promote flotation while ensuring a sufficient amount of charged groups to prevent coagulation. Achieving this balance remains a significant challenge in the development of effective NPs for mineral beneficiation. Without it, NP collectors still require high dosages due to their tendency to coagulate under flotation conditions and remain at the laboratory research stage. Researchers must first succeed in reducing dosage requirements and minimizing material waste to make NP collectors economically viable for commercial ores flotation.

Further studies are also needed for high-throughput screening of potential nanoparticle flotation collectors. These collectors offer specific advantages: firstly, when mineral surfaces are contaminated with nanoscale slimes, hydrophobic nanoparticles can outperform thin molecular collector layers, which can be buried beneath slime. This effect can be achieved by NPs deposition, inducing nanoscale roughness that creates an air/water interface characteristic of superhydrophobic surface. Secondly, this nanoscale roughness helps disrupt the thin water layer between very stable bubbles and mineral surfaces, facilitating direct contact. Overall, nanoparticles, are likely to be particularly useful in challenging systems where traditional collectors perform poorly.

## *2.3. Temperature responsive polymer (TRP)*

The most investigated temperature-responsive polymer applied in mineral processing is poly(N-isopropylacrylamide) (PNIPAM). Temperature, as an external stimulus, leads to reversible changes in the polymer microstructure, which refers to its unique ability for sol-gel transformation induced by temperature. There are two classes of thermo-responsive polymers: negative temperature-sensitive polymers, which are soluble at normal temperatures but become insoluble as the temperature increases and the lower critical solution temperature (LCST) is reached, with PNIPAM being an example; and positive temperature-sensitive polymers, which transform from miscible to insoluble as the solution temperature decreases to the upper critical solution temperature (UCST), with examples including polyacrylamide (PAAm), poly (acrylic acid) (PAA), and poly(acrylamide-*co*-butyl methacrylate) [67].

Thermo-responsive polymers hold promise in froth flotation, particularly for addressing challenges associated with fine valuable particles. These fine particles are not only difficult to recover but can also adhere to larger gangue particles as hydrophobic slime coatings, leading to a decrease in the quality of the recovered material. By using thermo-responsive polymers, these fine particles can be selectively aggregated into larger, hydrophobic flocs. This aggregation is facilitated by the polymer’s ability to transition between hydrophilic and hydrophobic states [68].

Below the LCST, the polymer amide group predominantly engages in hydrogen bonding with surrounding water. However, above the LCST, the energetically-preferred bonding with water diminishes, leading the NIPAM groups to form bonds with other NIPAM groups [69]. This causes the polymer chain to collapse into a globular structure, revealing the hydrophobic hydrocarbon backbone and precipitating out of solution (Fig. 10) [23].

The detailed description of the performance and characteristics of temperature-responsive polymers is provided in following sections and Table 3.

### 2.3.1. *Silica and quartz separation*

The first flotation tests with PNIPAM were conducted on silica/quartz [70–73] with comparisons made to kaolinite [70] and alumina [73]. In paper [70], Franks et al. proposed using PNIPAM as a multi-functional flotation reagent. At room temperature, it can act as a dispersant, but above its LCST, it behaves as a flocculant, collector, and frother.

The adsorption process begins to some extent at room temperature, where some PNIPAM molecules form hydrogen bonds with the oxide surface (e.g., silanol groups on silica). These pre-adsorbed polymeric molecules become hydrophobic above the LCST, thereby activating the hydrophobicity of the mineral surface. Adsorption continues onto the particle surfaces, likely forming multiple layers due to hydrophobic interactions. This results in hydrophobic attraction between particles, leading to the formation of hydrophobic flocs ready for flotation (Fig. 11) [70].

Silica recovery using only PNIPAM as a reagent can reach about 50 % after 5 min of flotation at 50 °C. The addition of 10 ppm of the frother (poly(propylene) glycol, or PPG) improves the recovery by 46 % [70]. Study [72] presented similar results with quartz flotation using only PNIPAM. The recovery with a single reagent with a molecular weight of 3.60 MDa was around 50 %. The authors also showed that recovery and contact angle increase with PNIPAM molecular weight, with the contact angle further increasing with temperature, changing from 42° at room temperature to 86° at 50 °C (for 3.60 MDa PNIPAM). Burdukova et al. [71] also concluded that the probability of particle/bubble attachment of quartz during flotation increases with the polymer's molecular weight and with temperatures above the LCST. This is evidenced by the increase in both the contact angle (indicating higher hydrophobicity) and the zeta potential (indicating lower repulsion from the electrical double layer) above the LCST.

In research [73], the authors improved PNIPAM selectivity by incorporating either a negative or a positive charge during the polymerization process using acrylic acid and di-methyl-amino-ethyl-acrylate, respectively. Cationic PNIPAM, compared to unmodified PNIPAM, improved quartz flotation recovery at 50 °C up to 67 %. However, the conventional collector DDA can achieve a quartz recovery of 90 %. For alumina, recovery with anionic PNIPAM showed good results, around 79 %. The polymer adsorption is induced by electrostatic interactions between the anionic polymer and positively charged alumina, and between the cationic polymer and negatively charged quartz.

### 2.3.2. *Kaolinite separation*

Franks et al. [70] presented the recovery results of kaolinite using PNIPAM as the collector. Without any reagent, the kaolinite recovery was 1 %. The addition of 20 ppm of PNIPAM and 10 ppm of PPG as a frother increased the recovery to 90 %. For comparison, hydrophobic flocculation–flotation was also performed using DDA (acting as both collector and frother) and polyacrylamide (PAM) as a flocculant. This conventional flocculation–flotation method achieved a lower recovery of around 78 %.

### 2.3.3. *Iron ore separation*

In study [74] researchers examined anionic PNIPAM with acrylic acid (PNIPAM-co-AA) as a potential iron ore collector, competing against the conventional hematite collector, sodium oleate (SO). The collectors were tested across three size ranges: coarse (+75 μm), mid-size (+20/−75 μm), and fines (−20 μm). PNIPAM-co-AA showed significantly better results than SO in recovering and concentrating particles from the mid-size and coarse fractions. With a dosage of 250 g/t, PNIPAM and SO achieved recoveries and grades for the coarse fraction at approximately 95 % and 87 % (recovery) and 37 % and 33 % (grade), respectively. In the mid-size fraction, PNIPAM achieved superior results with a dosage of 200 g/t, reaching approximately 95 % recovery and 83 % grade, whereas SO, even with higher dosages, yielded lower results at approximately 93 % recovery and 78 % grade. For fines particles, PNIPAM achieved 100 % recovery, but no selectivity occurred. SO showed some upgrading to a certain extent with lower dosages (150 and 250 g/t), with hematite grade being 10 % higher than in the feed; however, their recoveries reached only 61 % and 89 %. Overall, the polymer can produce a final concentrate with a higher grade than sodium oleate, while achieving similar or better recovery levels. Based on these results, the authors concluded that PNIPAM-co-AA is a better collector for particle sizes above 20 μm due to its lower sensitivity to fines and better selectivity and hydrophobicity in general. For particles smaller than 20 μm, sodium oleate offers better beneficiation, though with the loss of valuable fines in tailings, whereas PNIPAM recovered all fines but in an unselective manner due to gangue minerals entrapment during the flocculation process.

### 2.3.4. *Chalcopyrite and copper ore separation*

Studies [75,76] examined PNIPAM as a collector for chalcopyrite [75] and, further for copper ore with primary Cu-bearing minerals like chalcopyrite and bornite [76]. To increase PNIPAM selectivity towards copper sulfides during the free radical polymerization process, the authors created poly(NIPAM-*co*-ethyl xanthate methacrylate), referred to as PNEXMA in [75] and P(NIPAM-co-EXMA) in [76]. Notably, only 5 % mole xanthate was synthesized in both polymers.

Contact angle measurements showed that the addition of PAX or PNEXMA did not influence quartz hydrophilicity, likely due to the lack of collector adsorption on the mineral surface. With PAX and PNEXMA, chalcopyrite underwent hydrophobic modification, as indicated by an increase in contact angle across all dosages and temperatures. The high hydrophobicity of PNEXMA below the LCST might be due to metal xanthates and dixanthogen species formed on the chalcopyrite surface [75].

The synthetic mixture of chalcopyrite and quartz upgrading process in coarse and mid-size fractions showed results similar to PAX. Flotation conditions were the same for both polymeric and conventional

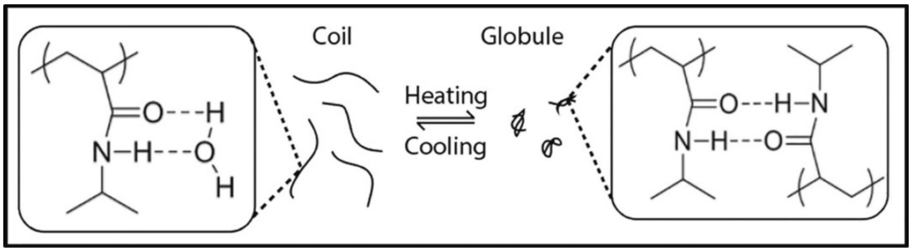

**Fig. 10.** The reversible hydrophilic-to-hydrophobic transition of PNIPAM upon heating above 32 °C in water [23] Copyright 2018 Elsevier Ltd.

**Table 3**
The temperature responsive polymers performance as collectors' and their adsorption characteristics (NG-not given).

| Polymers/ monomers used/ collector MW | Other agents used in polymerization process | Targeted mineral | Adsorption on mineral surface | Separation performance | Conventional performance (comparison) | Contact angle | Electrophoretic mobility (× $10^{-8}$ $m^2$ $s^{-1}$ $V^{-1}$) or Zeta potential | Reference |
|---|---|---|---|---|---|---|---|---|
| Poly(N-isopropylacrylamide) (PNIPAM)<br>MW = 0.23, 0.71, 2.0 and 3.6 MDa | None | Silica – silica powder (53 % of particle size <10 μm),<br>Kaolinite– pure mineral (particle size <10 μm with median particle size = 0.7 μm) | Below LCST some PNIPAM create hydrogen bonds with oxide surface (i.e. silanol groups on silica surface).<br>Above LCST PNIPAM strongly adsorbs onto the particle's surfaces, likely forming multiple layers driven by hydrophobic interactions. Since the molecules are hydrophobic after adsorbing on the particle surface, they activate the particle surface into a hydrophobic condition. Then hydrophobic attraction between particles induces flocculation into bigger hydrophobic flocs. | Frother poly(propylene) glycol (PPG) 10 ppm<br>10 ppm of PNIPAM at 50 °C:<br>Silica recovery ~96 %<br>Frother 10 ppm of PPG, 20 ppm of PNIPAM at natural pH 5.7 and 50 °C:<br>Kaolinite recovery ~90 % | 10 ppm of PAM (flocculant), 20 ppm of dodecyl amine hydrochloride (DDA) (collector) at pH 5.0 and 22 °C:<br>Kaolinite recovery ~78 % | NG | NG | [70] |
| PNIPAM<br>MW = 0.23, 1.32 and 4.5 MDa | None | Quartz – pure mineral (particles size 90–150 μm) | PNIPAM hydrophobic molecules have a very high affinity for quartz surfaces in aqueous medium. Above the LCST, PNIIPAM readily adsorbs onto quartz surfaces and creates dense, highly hydrophobic layer. | Poly (N-isopropylacrylamide) (PNIPAM) acts to enhance the probability of particle/bubble attachment at temperatures above the lower critical solution temperature (LSCT).<br>The resultant probability of particle/bubble attachment of quartz significantly increases with increasing molecular weight of PNIPAM. | NG | Temp. 22 °C:<br>Quartz θ = 4°<br>Quartz + PNIPAM θ = 28°<br>Temp. 50 °C:<br>Quartz θ = 4°<br>Quartz + PNIPAM θ = 71° | Zeta potential, at pH 8:<br>Temp. 22 °C:<br>Quartz: −61 mV<br>Quartz + PNIPAM: −47 mV<br>Temp. 50 °C:<br>Quartz: −50 mV<br>Quartz + PNIPAM: −36 mV | [71] |
| PNIPAM<br>MW = 0.23, 0.71, 2.0, 3.6, and 4.5 MDa | None | Silica - pure mineral (particles size <20 μm with 30 % below 5 μm) | NG | 20 ppm of 0.23/0.71/2/3.6 MDa PNIPAM at 50 °C, 5 min flotation time:<br>0.23 MDa PNIPAM:<br>Quartz recovery ~3 %/4 %/30 %/50 % | NG | Temp. 22 °C:<br>Quartz +0.23/ 0.71/2/3.6 MDa PNIPAM:<br>θ = 17°/ 26°/ 28°/42°<br>Temp. 50 °C:<br>Quartz +0.23/ 0.71/2/3.6 MDa PNIPAM:<br>θ = 49°/57°/ 72°/86° | NG | [72] |
| PNIPAM,<br>Acrylic acid,<br>Di-methyl-amino-ethyl-acrylate<br>Cationic PNIPAM MW = 1.18 MDa<br>Anionic PNIPAM = 1.84 MDa | None | Quartz - pure mineral (particles size 90–150 μm),<br>Alumina - pure mineral (particles size 90–150 μm) | Electrostatic interaction between anionic polymer to positively charged alumina and cationic polymer to negatively charged quartz. | 25 °C, 50 °C (conditioning) 50 °C (flotation)<br>1000 g/t of cationic (+) PNIPAM, at pH 8 and 50 °C (5 min):<br>Quartz recovery ~67 %<br>Alumina recovery ~22 %<br>1000 g/t of anionic (−) PNIPAM, at pH 8 and 50 °C:<br>Quartz recovery ~12 %<br>Alumina recovery ~79 % | Dodecyl amine (DDA):<br>Quartz recoveries ~90 % | NG | Zeta potential, at pH 8:<br>temp. 50 °C:<br>Quartz; −44 mV<br>Quartz + cationic/ anionic PNIPAM: −29 mV/ -48 mV<br>Alumina 9 mV<br>Alumina + cationic/anionic | [73] |

(*continued on next page*)

**Table 3** (*continued*)

| Polymers/ monomers used/ collector MW | Other agents used in polymerization process | Targeted mineral | Adsorption on mineral surface | Separation performance | Conventional performance (comparison) | Contact angle | Electrophoretic mobility (× $10^{-8}$ $m^2$ $s^{-1}$ $V^{-1}$) or Zeta potential | Reference |
|---|---|---|---|---|---|---|---|---|
| | | | | | | | PNIPAM: 11 mV/ −5 mV | |
| PNIPAM,<br>AA<br>PINPAM-co-AA MW = 4.5 MDa | None | Iron ore with hematite content of 56 %. (Coarse fraction >75 μm; Mids fraction 20–75 μm; Fine fraction 10–20 μm) | Electrostatic interaction between positively charged hematite an anionic polymer. | 25 °C (conditioning) → 50 °C (flotation)<br>**Coarse fraction** + 75 μm (feed grade: α = 27 %), at pH 8<br>150 g/t of PINPAM-co-AA: Hematite recovery; grade: ~45 %; ~87 %<br>200 g/t of PINPAM-co-AA: Hematite recovery; grade: ~66 %; ~68 %<br>250 g/t of PINPAM-co-AA: Hematite recovery; grade: ~95 %; ~37 %<br>**Mids fraction** 20–75 μm (α = 77 %), at pH 8<br>150 g/t of PINPAM-co-AA: Hematite recovery; grade: 83 ~ %; ~92 %<br>200 g/t of PINPAM-co-AA: Hematite recovery; grade: ~95 %; ~83 %<br>250 g/t of PINPAM-co-AA: Hematite recovery; grade:~100 %; ~76 %<br>**Fines fraction** 10–20 μm (α = 63 %), at pH 8<br>150 g/t of PINPAM-co-AA: Hematite recovery; grade: ~99 %; ~65 %<br>200 g/t of PINPAM-co-AA: Hematite recovery; grade: ~100 %; ~65 %<br>250 g/t of PINPAM-co-AA: Hematite recovery; grade:~100 %; ~62 %<br>**PINPAM-co-AA 150/200/250**<br>Total recovery: ~81 %/ ~94 %/ ~97 %<br>Total grade: ~86 %/ ~78 %/ ~63 % | **Coarse fraction**, at pH 8<br>150 g/t of Sodium oleate (SO): Hematite recovery; grade: ~55 %; ~45 %<br>250 g/t of SO: Hematite recovery; grade: ~87 %; ~33 %<br>750 g/t of SO: Hematite recovery; grade: ~98 %; ~27 %<br>**Mids fraction**, at pH 8<br>150 g/t of SO: Hematite recovery; grade: 80 ~ %; ~82 %<br>250 g/t of SO: Hematite recovery; grade: ~93 %; ~78 %<br>750 g/t of SO: Hematite recovery; grade:~100 %; ~77 %<br>**Fines fraction**, at pH 8<br>150 g/t of SO: Hematite recovery; grade: ~61 %; ~72 %<br>250 g/t of SO: Hematite recovery; grade: ~89 %; ~73 %<br>750 g/t of SO: Hematite recovery; grade:~94 %; ~65 %<br>**SO 150/250/750**<br>Total recovery: ~73 %/ ~91 %/ ~97 %<br>Total grade: ~73 %/ ~64 %/ ~56 % | NG | NG | [74] |
| PNIPAM,<br>2-Hydroxyethyl | 2,2′-Azobisisobutyronitrile (AIBN), | Chalcopyrite – pure mineral in synthetic | The xanthate functional group affinity for chalcopyrite. | 300 g/t of Poly(NIPAM-*co*-ethyl xanthate methacrylate) (PNEXMA) | 300 g/t of Potassium amyl xanthate | Temp. 22 °C; 50 °C: | NG | [75] |

(*continued on next page*)

**Table 3** (*continued*)

| Polymers/ monomers used/ collector MW | Other agents used in polymerization process | Targeted mineral | Adsorption on mineral surface | Separation performance | Conventional performance (comparison) | Contact angle | Electrophoretic mobility (× $10^{-8}$ $m^2 s^{-1} V^{-1}$) or Zeta potential | Reference |
|---|---|---|---|---|---|---|---|---|
| methacrylate (HEMA)<br>PNEXMA MW = 115 kDa | Tetrahydrofuran,<br>Carbon disulfide (CS$_2$),<br>Potassium hydroxide (KOH) | mixture with Quartz (particle size 36 % of coarse fraction >38 μm; 28 % of mids fraction 20–38 μm; 36 % of fines fraction <20 μm) | | at pH 9 (synthetic mixture chalcopyrite + quartz); 25 °C, 50 °C (conditioning) → 50 °C (flotation):<br>**Coarse fraction** + 38 μ:<br>Chalcopyrite recovery; grade: ∼98 %; ∼21 %<br>**Mids fraction** 20–38 μ:<br>Chalcopyrite recovery; grade: ∼100 %; ∼14 %<br>**Fines fraction** − 20 μ:<br>Chalcopyrite recovery; grade: ∼98 %; ∼7 % | (PAX), at pH 9:<br>**Coarse fraction** + 38 μ:<br>Chalcopyrite recovery; grade: ∼99 %; ∼20 %<br>**Mids fraction** 20–38 μ:<br>Chalcopyrite recovery; grade: ∼100 %; ∼14 %<br>**Fines fraction** − 20 μ:<br>Chalcopyrite recovery; grade: ∼95 %; ∼9 % | Quartz θ = 40°; 41°<br>Quartz + PAX θ = 32°; 33°<br>Quartz + PNEXMA θ = 40°; 31°<br>Chalcopyrite θ = 32°; 36°<br>Chalcopyrite + PAX θ = 71°; 80°<br>Chalcopyrite + PNEXMA θ = 67°; 70° | | |
| PNIPAM,<br>HEMA<br>P(NIPAM-co-EXMA)<br>MW = 1.5 MDa | tert-Butyl hydroperoxide (TBHP),<br>L-ascorbic acid,<br>THF,<br>CS$_2$,<br>KOH | Copper ore 0.67 % Cu grade, main minerals chalcopyrite and bornite (particle size 1 % of coarse fraction >38 μm; 24 % of mids fraction 20–38 μm; 75 % of fines fraction <20 μm) | The xanthate functional group affinity for chalcopyrite and bornite. | Mechanical flotation cell, 22.5 kg/t Cu of P(NIPAM-co-EXMA) at pH 9:<br>**Coarse + 20 μm** (α = 0.74 %)<br>25 °C (conditioning) → 50 °C (flotation):<br>Cu recovery, grade: ∼98 %; ∼18 %;<br>50 °C → 50 °C:<br>Cu recovery, grade: ∼98 %; ∼30 %;<br>**Fines − 20 μm** (α = 0.59 %)<br>25 °C → 50 °C:<br>Cu recovery, grade: ∼96 %; ∼6 %;<br>50 °C → 50 °C:<br>Cu recovery, grade: ∼98 %; ∼8 %;<br><br>Column flotation cell, 22.5 kg/t Cu of P(NIPAM-co-EXMA), 40 ppm of MIBC, at pH 9:<br>**Coarse + 53 μm** (α = 0.4 %)<br>25 °C → 50 °C:<br>7.5 kg/t; 22.5 kg/t Cu of P(NIPAM-co-EXMA)<br>Cu recovery, grade: ∼52 %, ∼7 %;: ∼56 %; ∼7 %;<br>50 °C → 50 °C:<br>22.5 kg/t Cu of P(NIPAM-co-EXMA):<br>Cu recovery, grade: ∼74 %; ∼18 %;<br>**Mids 20–53 μm** (α = 0.74 %)<br>25 °C → 50 °C:<br>7.5 kg/t; 22.5 kg/t Cu of P(NIPAM-co-EXMA)<br>Cu recovery, grade: ∼91 %, ∼16 %; ∼85 %; ∼9 %;<br>50 °C → 50 °C:<br>22.5 kg/t Cu of P(NIPAM-co-EXMA): | Mechanical flotation cell, 7.5 kg/t of PAX at pH 9:<br>**Coarse + 20 μm**<br>Cu recovery, grade: ∼91 %; ∼8 %;<br><br>**Fines + 20 μm**<br>Cu recovery, grade: ∼95 %; ∼4 %;<br><br>Column flotation cell, 7.5 kg/t of PAX, 40 ppm of MIBC, at pH 9:<br><br>**Coarse + 53 μm**<br>Cu recovery, grade: ∼68 %; ∼4 %;<br><br>**Mids 20–53 μm**<br>Cu recovery, grade: ∼91 %; ∼5 %; | NG | NG | [76] |

(*continued on next page*)

**Table 3** (*continued*)

| Polymers/ monomers used/ collector MW | Other agents used in polymerization process | Targeted mineral | Adsorption on mineral surface | Separation performance | Conventional performance (comparison) | Contact angle | Electrophoretic mobility (× $10^{-8}$ $m^2$ $s^{-1}$ $V^{-1}$) or Zeta potential | Reference |
|---|---|---|---|---|---|---|---|---|
| | | | | Cu recovery, grade: ∼88 %; ∼8 %;<br>**Fines – 20 μm** ($\alpha = 0.73$ %)<br>25 °C → 50 °C:<br>7.5 kg/t; 22.5 kg/t Cu of P(NIPAM-co-EXMA)<br>Cu recovery, grade: ∼95 %, ∼4 %; ∼90 %; ∼4 %;<br>50 °C → 50 °C:<br>22.5 kg/t Cu of P(NIPAM-co-EXMA):<br>Cu recovery, grade: ∼94 %; ∼3 % | **Fines – 20 μm**<br>Cu recovery, grade: ∼88 %; ∼3 %; | | | |
| PNIPAM,<br>N-acryloxysuccinimide (NASI)<br>(called TMP) | 2,2′-Azobis(2-methylpropionitrile),<br>2-(ethylthio)ethylamine (adjoin to TMPA),<br>4-benzil-3-thiosemicarbazide (adjoin to TMPB),<br>phosphine (adjoin to TMPPh) | Pyrite and (particles size 80–160 μm) pyrite with artificially coated gold (1700 ppm Au, particles size 40–80 μm).<br>Copper-nickel ore with Pt content.<br>Au—As ore, containing 3.5–3.6 ppm of gold. | The selective interaction of polymers with noble metals is provided due to the addition reaction of functional groups (thioamine, semicarbazide, and phosphine) to its molecule, capable to complexing with noble metals in the flotation conditions. | **Pyrite** flotation:<br>0,6 mg/L of TMPB, frother MIBK, temp. 40 °C:<br>Pyrite yield: ∼23 %<br>Pyrite with gold yield: ∼90 %<br>0,6 mg/L of TMPA, frother MIBK:<br>Pyrite yield: ∼15 %<br>Pyrite with gold yield: ∼92 %<br>**Cu—Ni ore** flotation, 100 g/t dimethyldithiocarbamate (DMDC), 10 g/t isopropyl xanthate (IKx), 4 g/t pine oil:<br>10 g/t DP-4 (collector) + 20 g/t of TMPA, temp. 40 °C:<br>Cu recovery 92 %,<br>Ni recovery 90 %;<br>Pt recovery 71 %,<br>Pd recovery 84 %<br>10 g/t DP-4 (collector) + 20 g/t of TMPPh, temp. 40 °C:<br>Cu recovery 93 %,<br>Ni recovery 90 %;<br>Pt recovery 75 %,<br>Pd recovery 82 %<br>**Au—As ore** flotation, 50 g/t of methylisobutylcarbinol (MIBC):<br>In total: 100 g/t of TMPA +150 g/t Butyl xanthate (ButX):<br>Au recovery 79 %,<br>In total: 100 g/t of TMPB +150 g/t ButX:<br>Au recovery 80 % | **Cu-Ni ore** flotation, 100 g/t DMDC, 10 g/t IKx, 4 g/t pine oil:<br>30 g/t DP-4 (collector):<br>Cu recovery 87 %,<br>Ni recovery 85 %;<br>Pt recovery 58 %,<br>Pd recovery 80 %<br>**Au—As ore** flotation, 50 g/t of MIBC:<br>In total: 250 g/t ButX:<br>Au recovery 75 % | NG | NG | [77] |
| Poly(ethylene glycol) methyl ether (PEG113-OH),<br>N-Isopropylacrylamide (NIPAM),<br>Glycidyl methacrylate (GMA) | 2,2′-Azobis (isobutyronitrile) (AIBN),<br>Rhodamine B thiohydrazide (RBS) | Au(III) from various metal ions solution.<br>Au(III) from the leaching solution of the printed circuit boards (PCBs). | Au(III) salt coordinates with N and S atoms in RBS and leads to the change of RBS structure. Incorporation of metal ions could open the spirolactam ring of RBS.<br>Fast adsorption of surfactant-Au(III) complex from the subsurface to the bubble | Metal ions solution flotation:<br>PEG-b-P(NIPAM-co-RBSG) at pH 7:<br>Au(III) recovery 85 %<br><br>PCBs leaching solution:<br>PEG-b-P(NIPAM-co-RBSG)<br>Au(III) recovery 81 %<br>Au(III) grade 35 % | NG | PEG-b-P (NIPAM-co-RBSG)<br>at 10 °C: θ = 85°<br>at 35 °C: θ = 135° | NG | [78] |

(*continued on next page*)

**Table 3** (*continued*)

| Polymers/ monomers used/ collector MW | Other agents used in polymerization process | Targeted mineral | Adsorption on mineral surface | Separation performance | Conventional performance (comparison) | Contact angle | Electrophoretic mobility ($\times 10^{-8}$ $m^2$ $s^{-1}$ $V^{-1}$) or Zeta potential | Reference |
|---|---|---|---|---|---|---|---|---|
| PEG-b-P(NIPAM-co-RBSG) MW = 16 kDa | | | surface occurs because of excellent hydrophobicity of polymeric surfactant and many hydrophobic sites of bubbles (hydrophobic-hydrophobic interaction). | | | | | |
| PEG,<br>PNIPAM,<br>HBMA | Aptamers P | Hg(II) | Interaction occurs due to the formation of Hg—N bond between Hg(II) ions and imide groups of aptamers. | TBC-P:<br>Hg(II) separation efficiency ~98 % | Aptamer P:<br>Hg(II) separation efficiency ~10 % | NG | NG | [79] |
| PNIPAM,<br>Chitosan (CS)<br>PNIPAM-CS MW = 3 kDa | *N,N*-methylenebisacrylamide (MBA),<br>Potassium persulfate (KPS),<br>Sodium dodecyl sulfate (SDS) | Ni(II)<br>Cr(VI) | The driving forces for adsorption of Ni(II) and Cr(VI) by PNIPAM-CS nano-hydrogels mainly involved electrostatic adsorption, ion exchange and complexation. The carboxyl and hydroxy groups in PNIPAM-CS nano-hydrogels had participated in the adsorption of heavy metal ions. The amide, hydroxyl and amino groups could be used as the ligands for collecting positively charged heavy metal ions through coordination and complexation. | Frother cocamidopropyl betaine (CAB) 70 mg/L, pH 6, temp. 313 K, PNIPAM-CS 6.0 g/L:<br>Ni(II) recovery 86 %<br>Cr(VI) recovery 92 % | Frother SDS 150 mg/L, pH 8.83, ethanol 6 % (*v*/v):<br>Ni(II) recovery 83 %<br>Cr(VI) recovery 67 % | NG | NG | [80]<br>Con. Perform.: [82] |
| N-Isopropylacrylamide (NIPAM),<br>1-vinylimidazole (1-VIM) | *N, N*′-methylenebisacrylamide (BIS),<br>2,2-azobis (2-methylpropionamidine) dihydrochloride (AIBA) | Cu(II) from salt solution containing Cu2+, Mg2+, Zn2+, Na+ | Cu2 + −imidazole complexation through nitrogen atoms. | Absorption capacity:<br>Cu(II) from pure Cu solution ~83 mg/g<br>Cu(II) from salt solution ~68 mg/g | NG | NG | Electrophoretic mobility at 70 °C<br>PNV0 = 5<br>PNV2 = 3.5<br>Below volume phase transition temperature (VPTT):<br>PNV0 ~ 32 °C,<br>PNV2 ~ 40 °C = 0 | [81] |

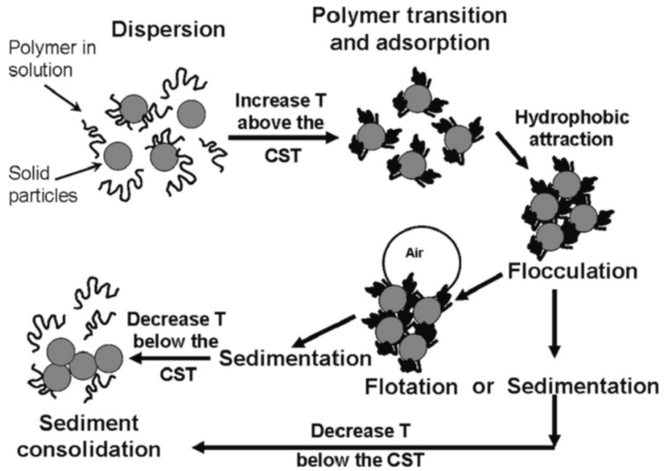

**Fig. 11.** Schematic illustration of the interactions between particles and PNIPAM in each step of the process comprising steps of dispersion, flocculation, flotation, sedimentation and sediment consolidation, [70]. Copyright 2009 Elsevier Ltd.

collectors, with a dosage of 300 g/t and pH equal to 9. Both collectors achieved recovery rates between 98 and 100 % in the coarse and mid-size fractions, with grades around 21 % and 14 %, respectively. In the fine fraction, both collectors enhanced beneficiation, with the polymeric collector achieving approximately 3 % better recovery, while PAX showed about 2 % better grade [75]. This phenomenon was also observed with an anionic PNIPAM and sodium oleate as collectors for iron ore [74], where the lower grade achieved with PNIPAM was suspected to be due to physical entrapment of gangue particles within the flocs.

Work [76] not only focused on comparing P(NIPAM-co-EXMA) and PAX for the flotation results of copper ore but also examined their performance in both mechanical and column flotation cells, as well as the effects of conditioning and flotation temperature. In the high-shear environment of a mechanical cell, P(NIPAM-co-EXMA) outperformed PAX in upgrading, achieving better recovery and significantly better grade in both coarse and fine fractions. Better results with the polymer were achieved at the same dosage of 7.5 kg/t Cu, with even higher results at three-fold the polymer dosage. In the low-shear column, the polymer's performance was comparable to PAX across all fractions, except for a much better performance with P(NIPAM-co-EXMA) at a higher dosage (22.5 kg/t Cu) and a conditioning and flotation temperature of 50 °C.

One observation by the authors suggested that polymer addition above the LCST potentially reduces its adsorption on quartz, improving its selectivity towards copper sulfides. This mechanism is likely due to micelle formation in the preheated suspension, where xanthate groups occupy the external structure and hinder polymer adsorption on gangue minerals. Another conclusion from this work suggests that P(NIPAM-*co*-EXMA) acts as a sulfide depressant at temperatures below the LCST because the adsorbed polymer does not transition into a hydrophobic state, preventing the particle-bubble attachment [76].

### 2.3.5. Noble metals separation

Temperature-responsive polymers can also be referred to as cloud point polymers. This term was used by Chanturia et al. [77]. The authors focused on the interaction mechanisms of these polymers with finely disseminated precious metal ores in flotation. The operating mechanism behind cloud point polymers is the same as that of thermo-responsive ones: at ambient temperature, the polymers are soluble, but upon heating, they become insoluble and acquire hydrophobic properties. The reagent is synthesized from N-isopropylacrylamide and N-acryloxysuccinimide, with the addition of functional groups from thioamine (TMPA), semicarbazide (TMPB), and phosphine (TMPPh). These groups are capable of complexing with noble metals under flotation conditions [77].

Cloud point polymers TMPA and TMPB were used as collectors in flotation of pyrite artificially coated with gold (pyrite-Au). Both polymers yielded positive results, with pyrite-Au recovery around 90 %. In the case of copper-nickel ore with Pt content and Au—As ore, cloud point polymers were used as co-collectors at different stages of the flotation scheme. The use of these polymers improved flotation process efficiency by decreasing the loss fraction of fine grains to 16–25 %. Additionally, they enhanced the performance of conventional collectors by increasing the recovery of noble metals between 2 and 17 % [77].

Wang et al. [78] presented the application of a thermo-responsive amphiphilic polymer, poly(ethylene glycol)-b-poly(N-isopropylacrylamide-co-glycidyl methacrylate) ($PEG_{113}$-b-P($NIPAM_{108}$-co-$GMA_{62}$)), with rhodamine B thiohydrazide (RBS) as a collector for Au(III) ions from secondary resources. Au(III) salts are coordinated with the N and S atoms in RBS, which enhances the polymer's selectivity towards Au. Due to the excellent hydrophobicity of the GMA moieties, the surfactant-Au(III) complex adsorbs quickly onto bubbles through hydrophobic-hydrophobic interaction (Fig. 12). The recovery of Au(III) salts reached 85 % from artificially prepared solution, and from the leaching solution of printed circuit boards (PCBs), 81 %, with the Au(III) grade increasing from 2 % to 35 %.

Moreover, the polymer-Au(III) complex solution can be regenerated using oxalic acid to release Au(III). Further heating and drying yielded a polymeric reagent that forms a micelle structure upon heating, due to the presence of both hydrophilic P($NIPAM_{108}$-*co*-$RBSG_3$) and hydrophobic $PEG_{113}$ chains. The regenerated polymer maintained a separation efficiency level above 80 % even after five cycles of regeneration [78].

### 2.3.6. Ions' separation

In work [79], the utilization of aqueous two-phase flotation (ATPF) with aptamer-functionalized thermo-responsive polymers as collectors was described. The synthesized collector, PEG113-b-P(NIPAM90-co-HBMA3)-P (TBC—P), shows selectivity towards Hg(II) ions through reversible coordination interactions provided by the aptamer. These interactions occur due to the formation of Hg—N bonds between Hg(II) ions and the imide groups of the aptamers. Under optimal separation conditions, a 97 % separation efficiency of Hg(II) ions can be achieved. In contrast, aptamer-Hg(II) complexes are unable to attach to bubbles and float, resulting in low recovery.

The two-phase system and the properties of the polymer allow for the recycling of the aptamer-functionalized thermo-responsive polymeric collector. The first phase, consisting of Hg(II) ions, the TBC-P collector, and a solution of $K_3C_6H_5O_7$ (or $KH_2PO_4$), is where flotation occurs. The second phase, made of PEG-10000, is used for extracting the TBC-P-Hg (II) complexes. Due to the ability of PNIPAM to transform into an insoluble solid state upon heating, the complex is retrieved from the PEG-10000 solution. Cysteine (Cys) is then used to release Hg(II) ions from the TBC-P-Hg(II) complexes. After another heating, followed by filtration and drying, the collector is recycled for further utilization [79].

Work [80] tested PNIPAM-chitosan intelligent nano-hydrogels as collectors for the recovery of Ni(II) and Cr(VI) ions. Under acidic conditions, Cr(VI) mainly existed in the anionic form HCrO4-, while Ni(II) ions were in the cationic form. The adsorption of Ni(II) and Cr(VI) by PNIPAM-CS nano-hydrogels was generally achieved through electrostatic adsorption, ion exchange, and complexation. The carboxyl and hydroxy groups in PNIPAM-CS nano-hydrogels participated in the adsorption of heavy metal ions. The amide, hydroxyl, and amino groups collected positively charged heavy metal ions through coordination and complexation. The recoveries of Ni(II) and Cr(VI) were 86 % and 92 %, respectively, whereas conventional reagents like ethanol (collector) and SDS (frother) achieved lower recoveries of around 83 % and 67 %, respectively. During the experiments, it was observed that the chitosan

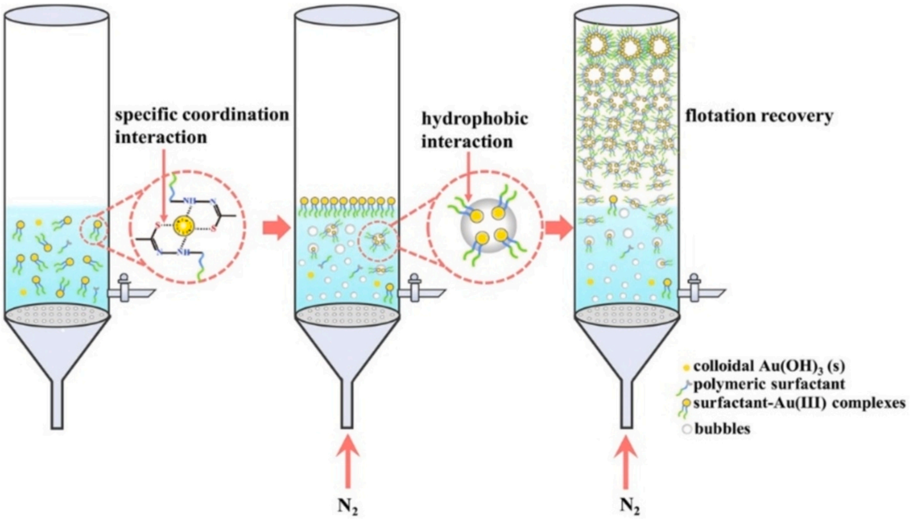

**Fig. 12.** The mechanism for flotation recovery of Au(III) salt by polymeric surfactant [78]. Copyright 2023 Elsevier B.V.

content in the nano-hydrogel influenced the phase transition behaviors and increased the final LCST of the hydrogel.

This study [81] introduces a new concept of using ion-complexation to control the responsiveness of microgels, which in turn stabilizes foams and emulsions. The findings lay the groundwork for developing a responsive flotation method for selective $Cu^{2+}$ recovery in a single step. This approach promises advantages over traditional treatment methods in terms of efficiency, circular economy, and simplicity.

The p(NIPAM-co-VIM) microgel (PNV2) showed excellent selectivity for $Cu^{2+}$ ions in solutions that also contained competing ions such as $Na^+$, $Mg^{2+}$, and $Zn^{2+}$. It demonstrated a strong capacity to absorb $Cu^{2+}$, with approximately 82.6 mg/g in pure $Cu^{2+}$ solutions and about 67.7 mg/g in the presence of mixed competitive ions. The p(NIPAM-co-VIM) microgel forms $Cu^{2+}$ complexes through imidazole groups. The microgel maintained its ability to swell in mixed salt solutions (Fig. 13), although the volume phase transition temperature (VPTT) value was balanced by $Zn^{2+}$-amide complexation. Additionally, the stability of $Cu^{2+}$-tunable foam was preserved in these mixed salt solutions [81].

### 2.3.7. *Summary*

Thermo-responsive polymers offer several advantages in mineral flotation. They can selectively aggregate fine particles, enhancing recovery. Their selectivity can be adjusted through the addition of extra monomers or other reagents in the polymerization process to incorporate specific functional groups. Similar to nanoparticles they can adsorb onto minerals through electrostatic interactions, coordination, or complexation. After heating above the lower critical solution temperature (LCST), hydrophobic interactions also come into play. This ability to transition from a hydrophilic to a hydrophobic state makes them versatile for various mineral separation processes and conditions, serving as a good alternative to conventional chemical reagents. The transition not only helps increase the recovery of valuable fines but also facilitates the recovery of the polymer itself.

However, thermo-responsive polymers also have some drawbacks. Incorporating additional monomers and reagents into the polymer core can alter its LCST, usually increasing it, which leads to higher energy consumption costs. Another still unsolved challenge is the entrapment of gangue fines during the flocculation process above the LCST.

## 2.4. *Block copolymers (BcP)*

The block copolymers presented in this chapter for mineral processing purposes are amphiphilic, meaning their molecules exhibit affinity towards two distinct environments. Their amphiphilic nature is

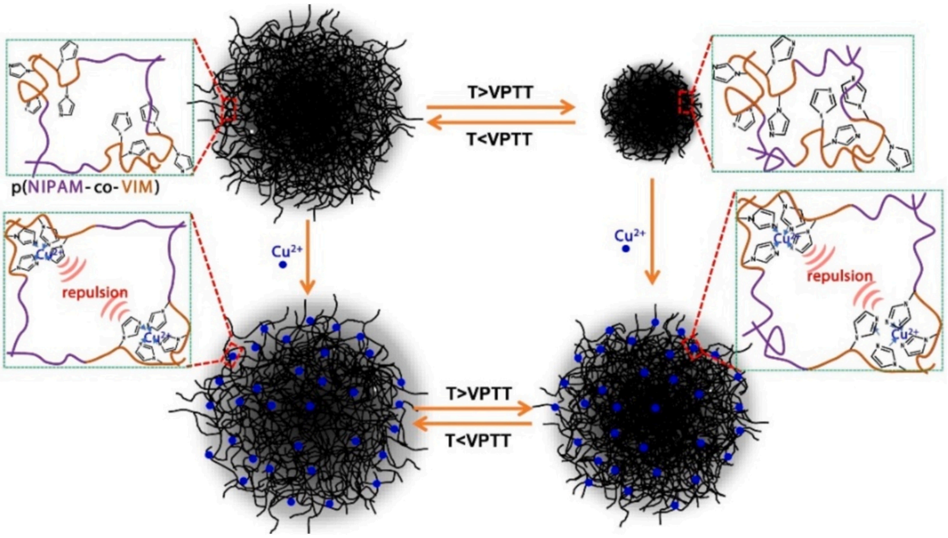

**Fig. 13.** Effect of $Cu^{2+}$ complexation on swelling property of PNV microgel [81]. Copyright 2022 Elsevier B.V.

similar to that of surfactants, where one building monomer is hydrophilic (capable of carrying a charge) and the other is hydrophobic. Block copolymers can self-assemble and form different morphologies; for example, when dissolved in a selective solvent, they can form micelles [83]. Block copolymers can be an alternative to temperature-responsive polymers, where the hydrophilic-hydrophobic transition needs to be induced by heating. This is beneficial as inducing such transitions through heating on an industrial scale would lead to increased costs [84].

In both papers [24,84], poly n-butyl acrylate (PBA) was used as the hydrophobic monomer with varying lengths, while the length of the hydrophilic monomer remained constant. The method used to synthesize these diblock copolymers was reversible addition−fragmentation chain-transfer (RAFT) mediated emulsion polymerization.

The detailed description of the performance and characteristics of block copolymers is provided in following sections and Table 4.

### 2.4.1. *Magnesium hydroxide separation*

In study [84], amphiphilic poly(acrylic acid)-b-poly(n-butyl acrylate) (PAA-PnBA) was investigated for its dual role as a flocculant and a collector. Its adsorption on mineral surfaces can occur in two ways: as individual copolymer chains through the negatively charged hydrophilic PAA block, facilitating charge patch flocculation below the critical micelle concentration (CMC), or as micelles above the CMC, enabling micellar adsorption and pseudo-bridging flocculation (Fig. 14). In this latter case, the exposed hydrophobic tails on the particle surface form hydrophobic layers.

The conventional collector, sodium dodecyl sulfate (SDS), outperformed all three block copolymers variations in the flotation recovery of $Mg(OH)_2$, achieving a recovery rate of 93 %, although it required a much higher concentration of reagent. Among the block copolymers, the highest recovery was achieved by the largest molecular weight $PAA_{153}$-b-$PnBA_{200}$, with a recovery rate of around 52 %. The intermediate molecular weight $PAA_{153}$-b-$PnBA_{100}$ showed a recovery of approximately 32 %, while the smallest hydrophobic block polymer, $PAA_{153}$-b-$PnBA_{25}$, achieved a maximum recovery of about 30 % [84].

In comparison, SDS, at a concentration similar to that at which the polymers achieved their highest performance (about 20 μM), recovered only about 53 % of $Mg(OH)_2$. The $PAA_{153}$-b-$PnBA_{200}$ exhibited superior collection efficiency, outperforming the conventional reagent SDS, but only below its micellar adsorption transition point. Beyond the CMC, the hydrophobisation of $Mg(OH)_2$ particles and their floatability decreased due to the low surface energy of the created polymeric micelles and the lack of exposed hydrophobic chains. Large flocs were unable to form stable aggregates with bubbles; however, combined flotation-sedimentation operations would settle them in the next clarification step. The pseudo-bridging flocculation regime demonstrated excellent settling rates before flotation, and post-flotation sedimentation is anticipated to significantly reduce the solids concentration in the cell. This suggests that these amphiphilic block copolymers have strong potential for the rapid dewatering of radioactive and other mineral wastes [84].

### 2.4.2. *Quartz separation*

In paper [24], copolymers consisting of a hydrophilic block of poly dimethylaminoethyl acrylate quaternised with methyl iodide ($PDMAEAI^+$) with cationic charge and a hydrophobic poly n-butyl acrylate (PBA) were tested as flotation collectors for quartz. The cationic character of $PDMAEAI^+$, attributed to its polar quaternised functional group, acts as an active receptor-ligand targeting the quartz surface and adsorbing onto it. At a concentration of $3 \times 10^{-5}$ mol/L, the final quartz recoveries obtained by the copolymers $PDMAEAI^+_{10}$-$PBA_{10}$, $PDMAEAI^+_{10}$-

**Table 4**

The block copolymers collectors' performance and adsorption characteristics (NG-not given).

| Polymers/ monomers used | Targeted mineral | Adsorption on mineral surface | Separation performance | Conventional performance (comparison) | Contact angle | Reference |
|---|---|---|---|---|---|---|
| Acrylic acid (AA),<br>n-butyl acrylate (nBA) | Magnesium hydroxide, $Mg(OH)_2$ | The initial electrostatic adsorption and relaxation of unimer block copolymers onto the particle surface driven by the PAA block, followed by potential relaxation and hydrophobic adsorption of the hydrophobic PnBA tails to the charge neutralized sites on the particle surface. | Frother: 98 µM MIBC<br>15 µM of PAA153-b-PnBA200<br>$Mg(OH)_2$ recovery 52 %<br>20 µM of PAA153-b-PnBA100<br>$Mg(OH)_2$ recovery 32 %<br>2 µM of PAA153-b-PnBA25<br>$Mg(OH)_2$ recovery 30 % | Frother: 98 µM MIBC<br>20 µM of SDS:<br>$Mg(OH)_2$ recovery ~53 %<br>900 µM of SDS:<br>$Mg(OH)_2$ recovery 93 % | NG | [84] |
| Poly dimethylaminoethyl acrylate quaternised with methyl iodide (PDMAEAI+),<br>Poly n-butyl acrylate (PBA)<br>PBA10 MW = 4.4 kDa<br>PBA20 MW = 5.7 kDa<br>PBA30 MW = 7.0 kDa | Quartz - pure mineral (80 % particles <75 µm) | Cationic character of PDMAEAI+, due to polar quaternised functional group as active receptor-ligand targeting the quartz surface. | Concentration $1 \times 10^{-5}$ mol/L, pH 10.5<br>PBA10<br>Quartz recovery ~79 %<br>PBA20<br>Quartz recovery ~80 %<br>PBA30<br>Quartz recovery ~83 %<br>Concentration $3 \times 10^{-5}$ mol/L, pH 10.5<br>PBA10, PBA20, PBA30<br>Quartz recovery ~94 % | Concentration $1 \times 10^{-5}$ mol/L of dodecylamine (DDA)<br>Quartz recovery ~25 %<br>Concentration $3 \times 10^{-5}$ mol/L, pH 10.5<br>Quartz recovery ~35 %<br>Concentration $9\times 10^{-5}$ mol/L of DDA<br>Quartz recovery ~90 % | Quartz:<br>θ = 20°<br>Quartz + PBA10<br>θ = 84°<br>Quartz + PBA20<br>θ = 91°<br>Quartz + PBA30<br>θ = 93°<br>Quartz + DDA<br>θ = 32° | [24] |

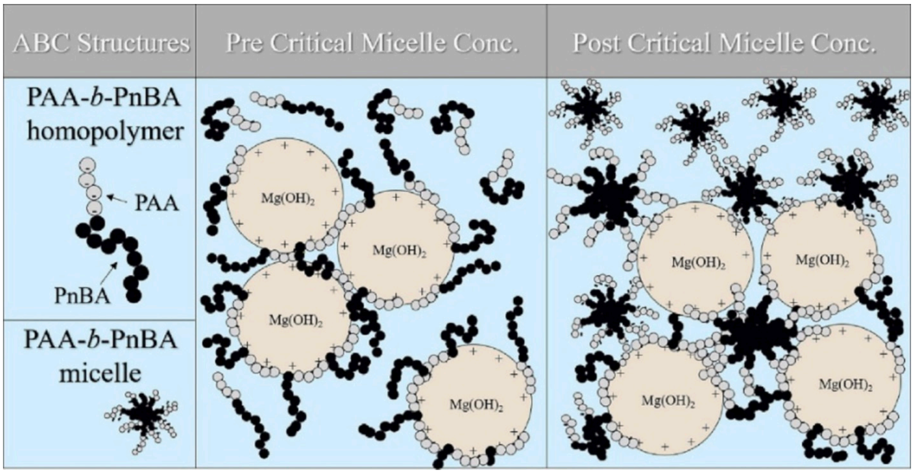

**Fig. 14.** Illustration of the change in adsorption and flocculation mechanisms pre and post critical micelle concentrations (CMC) of the amphiphilic block copolymers [84] CC BY 4.0 license.

$PBA_{20}$, and $PDMAEAI^+_{10}$-$PBA_{30}$ were approximately 94 %. In contrast, at the same concentration, dodecylamine (DDA) reached only 35 % recovery. To achieve a quartz recovery of up to 90 % with DDA, the concentration needed was three times higher than that required for the polymers. There is a correlated increase in contact angle values and the number of PBA groups, corresponding to the increase in surface hydrophobisation. However, with a higher number of PBA hydrophobic groups, the solubility of the collector decreased, as did its foamability and foam stability. These parameters can all be controlled by manipulating the number of PBA groups, demonstrating the significant potential of these polymers in mineral flotation.

### 2.4.3. *Summary*

Block *co*-polymers are another competitive alternative to conventional collectors. By copolymerizing different monomers and controlling their molecular weights, designers can tailor the functionality of these collectors. Additionally, some monomers can also serve as frothers, adding an extra function to the reagent.

## 3. Conclusions

Polymers as collectors are a relatively new concept in the field of mineral flotation and currently exist mainly in experimental and theoretical studies. However, this approach is a promising direction for finding greener alternatives to conventional chemical reagents. Interest in this topic began in the 2000s and continues to attract more research capacity today.

The possibilities of building different polymers are virtually endless, only restricted by chemical and thermodynamic laws [85]. This diversity is reflected in the various types of polymeric collectors tested in flotation applications, such as conventional polymers, nanoparticles, temperature-responsive polymers, and block copolymers. These polymers not only utilize their natural properties for the recovery of minerals and metal ions but also incorporate functionalities from other reagents.

Utilizing conventional polymers as collectors, such as poly(propylene glycol) bis(2-aminopropyl ether) (PEA), poly(amidoamine) (PAMAM), and β-Cyclodextrin (β-CD), can lead to a beneficial, more environmentally friendly shift. These polymers exhibit low toxicity and minimal environmental impact, making them attractive alternatives in flotation processes. Even the use of toxic poly(oxyethylene) nonylphenyl ether (PONPE) in ion flotation can have a positive outcome by eliminating the chemicals used in conventional solvent extraction for ions.

Tabular summaries in each section (Tables 1–4) demonstrate the promising performance of polymeric collectors, often outperforming traditional ones in many cases. However, some disadvantages also highlight the need for further improvement. In the case of nanoparticles, a significant issue is their much higher dosage compared to traditional collectors. This problem arises due to the high ionic strength of the flotation pulp, which causes nanoparticles to coagulate. Consequently, achieving high efficiency with nanoparticles requires increased dosages. Researchers need to further investigate the balance between the charge of nanoparticles and their hydrophobicity to optimize their performance and reduce the required dosages for successful flotation. A positive aspect of utilizing nanoparticles as collectors is their effective performance in the presence of slime. The larger size of nanoparticles helps to create particle-bubble aggregates where conventional collectors are insufficient and often hindered by slime coating.

Despite the considerable potential of NPs collectors, their widespread utilization may be hindered by the distribution of petroleum-based microplastics in the aqueous phase, which can be considered a significant drawback of the proposed idea. In recent years, nano/microplastics from non-biodegradable and non-sustainable petro-polymers (i.e., PP, PE, PVC, PET, etc.) have garnered growing public concern due to their widespread distribution and harmful impacts. Their distinctive features, including porous structure, small size, and large specific surface area, have been identified as the main reasons for the harmful effects of synthetic microplastics on living organisms [86]. Therefore, considering the significant advantages of these types of flotation reagents, all efforts should be directed towards designing NPs made of fully biodegradable and biocompatible biopolymers, possibly of bacterial origin, such as polyhydroxyalkanoates.

A shortcoming of PNIPAM-based temperature-responsive polymeric collectors is the need to heat the pulp for flotation to occur. However, their performance often surpasses that of conventional collectors, even at the same or lower dosages. The higher energy costs could be offset by reduced reagent consumption and improved recovery of valuable fines, which typically end up in tailings due to their insufficient size to float with conventional chemical reagents. Additionally, the lower critical solution temperature (LCST) of PNIPAM can be decreased by incorporating hydrophobic monomers into its structure [87], potentially reducing heating costs.

Moreover, PNIPAM is extensively studied in various biomedical fields, including tissue engineering, drug delivery systems, and wound dressings, demonstrating its nontoxicity and biodegradability [88]. A notable advantage of utilizing PNIPAM is its application in aqueous two-phase flotation (ATPF). In this process, the phase transition of the PNIPAM component of the collector can be leveraged to recycle the collector for further use in the flotation process.

Block copolymers are a good alternative to temperature-responsive polymeric collectors. Their amphiphilic structure provides hydrophilic monomers for adsorption sites on mineral particles and hydrophobic monomers to enhance particle-bubble attachment. However, the design process needs to carefully control the molecular weight and chain length of both polymers due to their natural tendency to form micelles. Above their critical micelle concentration, increased micelle formation can prevent effective flotation.

The advantage of using polymeric collectors lies in their significantly lower toxicity, or in many cases, their complete lack thereof. In several examples discussed in this review, the authors employed environmentally benign cores with incorporated affinity towards specific minerals, derived from chemical reagents during the polymerization process. This approach enables the reduction of conventional collector dosages while preserving effectiveness.

Further research is needed to design a comprehensive library of polymers suitable for specific mineral collection at the laboratory scale, while also being effective in scaling up for industrial trials. Tests on natural ore that simulate processing plant environments are crucial for enabling the transition from conventional chemical reagents to greener polymeric collectors. The cited research indicates that natural polymers such as lignin, chitin, chitosan, and dextrin can perform as well as synthetic ones like polystyrene, PNIPAM, and poly(butyl acrylate). The benefits of exploring natural polymers—namely their biodegradability, non-toxicity, and renewability—not only highlight their performance potential but also align with environmental sustainability goals, making them a promising focus for future research. Achieving this goal requires a combination of various knowledge areas, including polymer and surface chemistry, material science, chemical engineering, flotation technology, mineralogy, and environmental science.

## CRediT authorship contribution statement

**Patrycja S. Bednarek:** Visualization, Validation, Software, Investigation, Formal analysis, Data curation, Conceptualization, Writing – original draft. **Przemyslaw B. Kowalczuk:** Supervision, Project administration, Funding acquisition, Conceptualization, Writing – review & editing. **Jan Zawala:** Writing – review & editing.

## Declaration of competing interest

The authors declare that they have no known competing financial interests or personal relationships that could have appeared to influence the work reported in this paper.

## Data availability

Dataverse

## References

[1] Nagaraj DR, Farinato RS. Evolution of flotation chemistry and chemicals: a century of innovations and the lingering challenges. Miner Eng 2016;96-97:2–14. https://doi.org/10.1016/j.mineng.2016.06.019.

[2] Chander S, Nagaraj DR. FLOTATION | Flotation reagents. Elsevier; 2007. p. 1–14.

[3] Wills BA, Finch JA. Froth flotation. Elsevier; 2016. p. 265–380.

[4] Bulatovic SM. Classification of flotation reagents. Elsevier; 2007. p. 1–3.

[5] Drzymała J. Mineral processing: Foundations of theory and practice of minerallurgy. 1st ed. Wroclaw, Poland: Oficyna Wydawnicza Politechniki Wroclawskiej; 2007.

[6] Bulatovic SM. Use of organic polymers in the flotation of polymetallic ores: a review. Miner Eng 1999;12:341–54. https://doi.org/10.1016/s0892-6875(99)00015-1.

[7] Wang D. Introduction. Springer Singapore; 2016. p. 1–8.

[8] Bednarek PS. Supplementary Data for: Polymer-based collectors in flotation: A review. In: Science NNUo, Technology, editor. DataverseNO; 2024. https://doi.org/10.18710/IUHE48.

[9] Forbes E. Shear, selective and temperature responsive flocculation: a comparison of fine particle flotation techniques. Int J Miner Process 2011;99:1–10. https://doi.org/10.1016/j.minpro.2011.02.001.

[10] Asgari K, Khoshdast H, Nakhaei F, Garmsiri MR, Huang Q, Hassanzadeh A. A review on floc-flotation of fine particles: technological aspects, mechanisms, and future perspectives. Miner Process Extr Metall Rev 2023:1–28. https://doi.org/10.1080/08827508.2023.2236770.

[11] Tian J, Gao H, Guan J, Ren Z. Modified floc-flotation in fine sericite flotation using polymethylhydrosiloxane. Sep Purif Technol 2017;174:439–44. https://doi.org/10.1016/j.seppur.2016.10.051.

[12] Ding KJ, Laskowski JS. Effect of conditioning on selective flocculation with polyacrylamide in the coal reverse flotation. Miner Process Ext Metall 2007;116: 108–14. https://doi.org/10.1179/174328507x163797.

[13] Li M, Xiang Y, Chen T, Gao X, Liu Q. Separation of ultra-fine hematite and quartz particles using asynchronous flocculation flotation. Miner Eng 2021;164:106817. https://doi.org/10.1016/j.mineng.2021.106817.

[14] Mei Y, Lin Q, Wu C, Huang W, Cao D, Liu K. Efficient separation of ultrafine coal assisted by selective adsorption of Polyvinylpyrrolidone. Minerals 2022;12:725. https://doi.org/10.3390/min12060725.

[15] Warren LJ. Shear-flocculation of ultrafine scheelite in sodium oleate solutions. J Colloid Interface Sci 1975;50:307–18. https://doi.org/10.1016/0021-9797(75)90234-9.

[16] Zhou S, Wang X, Bu X, Wang M, An B, Shao H, et al. A novel flotation technique combining carrier flotation and cavitation bubbles to enhance separation efficiency of ultra-fine particles. Ultrason Sonochem 2020;64:105005. https://doi.org/10.1016/j.ultsonch.2020.105005.

[17] Huang G, Xu J, Geng P, Li J. Carrier flotation of low-rank coal with polystyrene. Minerals 2020;10:452. https://doi.org/10.3390/min10050452.

[18] Zhang X, Hu Y, Sun W, Xu L. The effect of polystyrene on the carrier flotation of fine Smithsonite. Minerals 2017;7:52. https://doi.org/10.3390/min7040052.

[19] Scharnberg A, Oliveira H, Weschenfelder S, Rubio J, Azevedo A. Flocculation of emulsified oil-in-water with dodecylbenzene sulfonate and polyacrylamide and floc separation by dissolved air flotation. Colloids Surf A Physicochem Eng Asp 2023;669:131496. https://doi.org/10.1016/j.colsurfa.2023.131496.

[20] Rocha E, Silva FCP, Silva Rocha E, NMP, Luna JM, Rufino RD, Santos VA, Sarubbo LA.. Dissolved air flotation combined to biosurfactants: a clean and efficient alternative to treat industrial oily water. Rev Environ Sci Biotechnol 2018;17: 591–602. https://doi.org/10.1007/s11157-018-9477-y.

[21] Demir-Yilmaz I, Ftouhi MS, Balayssac S, Guiraud P, Coudret C, Formosa-Dague C. Bubble functionalization in flotation process improve microalgae harvesting. Chem Eng J 2023;452:139349. https://doi.org/10.1016/j.cej.2022.139349.

[22] Woodard Curran I. Methods for treating wastewaters from industry. Elsevier; 2006. p. 149–334.

[23] Ng WS, Connal LA, Forbes E, Franks GV. A review of temperature-responsive polymers as novel reagents for solid-liquid separation and froth flotation of minerals. Miner Eng 2018;123:144–59. https://doi.org/10.1016/j.mineng.2018.03.027.

[24] Chimonyo W, Peng Y. Evaluation of novel RAFT block copolymers as alternatives to amine collectors. Miner Eng 2023;193:108020. https://doi.org/10.1016/j.mineng.2023.108020.

[25] Drzymala J, Kowalczuk P. Classification of flotation frothers minerals8; 2018. p. 53. https://doi.org/10.3390/min8020053.

[26] Kowalczuk PB, Zawala J, Kosior D, Drzymala J, Malysa K. Three-phase contact formation and flotation of highly hydrophobic polytetrafluoroethylene in the presence of increased dose of Frothers. Ind Eng Chem Res 2016;55:839–43. https://doi.org/10.1021/acs.iecr.5b04293.

[27] Khoshdast H, Hassanzadeh A, Kowalczuk PB, Farrokhpay S. Characterization techniques of flotation Frothers - a review. Miner Process Extr Metall Rev 2023;44: 77–101. https://doi.org/10.1080/08827508.2021.2024822.

[28] Sobouti A, Rezai B, Hoseinian FS. A review of the application of nanoparticles as collectors in ion flotation. Physicochem Probl Miner Process 2023. https://doi.org/10.37190/ppmp/176040.

[29] Peng W, Chang L, Li P, Han G, Huang Y, Cao Y. An overview on the surfactants used in ion flotation. J Mol Liq 2019;286:110955. https://doi.org/10.1016/j.molliq.2019.110955.

[30] Saim AK. Recent Progress in the application of nanoparticles in minerals flotation. Chem Sci Eng Res 2021;3:1–7. https://doi.org/10.36686/Ariviyal.CSER.2021.03.06.027.

[31] Cheng G, Xiong L, Lu Y, Zhang ZG, Lv C, Lau EV. Advancements in the application of surface roughness in mineral flotation process. Sep Sci Technol 2024;59: 592–611. https://doi.org/10.1080/01496395.2024.2329789.

[32] Wei M, Ban B, Li J, Sun J, Li F, Jiang X, et al. Flotation behavior, collector adsorption mechanism of quartz and feldspar-quartz systems using PEA as a novel green collector. Silicon 2020;12:327–38. https://doi.org/10.1007/s12633-019-00135-3.

[33] Li J, Lin Y, Shi J, Ban B, Sun J, Ma Y, et al. Recovery of high purity Si from kerf-loss Si slurry waste by flotation method using PEA collector. Waste Manag 2020;115: 1–7. https://doi.org/10.1016/j.wasman.2020.07.023.

[34] Jiang X, Shi J, Chen C, Song W, Ban B, Li J, et al. Flotation mechanism and application of PEA with different chain lengths in quartz flotation. Chem Eng Sci 2021;246:116813. https://doi.org/10.1016/j.ces.2021.116813.

[35] Mo Z, Zhu X, Jiang X, Ding J, Wang L, Ban B, et al. Study on the flotation behavior and mechanism of glass Fiber powder. Silicon 2024. https://doi.org/10.1007/s12633-024-02984-z.

[36] Safety Data Sheet. Poly(propylene glycol) bis(2-aminopropyl ether), Sigma Aldrich. Accessed 24th May. 2024.

[37] Şener M, Gültek A. Magnetite flotation from Sanidine with environmental benign collector poly(Amidoamine). Min Metall Explor 2023;40:913–22. https://doi.org/10.1007/s42461-023-00751-z.

[38] Kinoshita T, Ishigaki Y, Shibata N, Yamaguchi K, Akita S, Kitagawa S, et al. Selective recovery of gallium with continuous counter-current foam separation and

its application to leaching solution of zinc refinery residues. Sep Purif Technol 2011;78:181–8. https://doi.org/10.1016/j.seppur.2011.01.044.

[39] Safety Data Sheet. Polyoxyethylene(20) Nonylphenyl Ether, FUJIFILM Wako Chemical Corporation. Accessed 28th May. 2024.

[40] Kinoshita T, Akita S, Nii S, Kawaizumi F, Takahashi K. Solvent extraction of gallium with non-ionic surfactants from hydrochloric acid solution and its application to metal recovery from zinc refinery residues. Sep Purif Technol 2004; 37:127–33. https://doi.org/10.1016/j.seppur.2003.09.003.

[41] Kinoshita T, Ishigaki Y, Shibata N, Akita S, Kondou H, Nii S. Selective recovery of gold(III) via continuous counter-current foam separation from hydrochloric acid solution – effects of foam and column sizes on separation performance. Sep Purif Technol 2013;116:335–41. https://doi.org/10.1016/j.seppur.2013.06.012.

[42] Kozlowski CA, Girek T, Walkowiak W, Kozlowska J. The effect of β-CD polymers structure on the efficiency of copper(II) ion flotation. J Incl Phenom Macrocycl Chem 2006;55:71–7. https://doi.org/10.1007/s10847-005-9020-y.

[43] Yang S, Pelton R, Raegen A, Montgomery M, Dalnoki-Veress K. Nanoparticle flotation collectors: mechanisms behind a new technology. Langmuir 2011;27: 10438–46. https://doi.org/10.1021/la2016534.

[44] Yang S, Pelton R. Nanoparticle flotation collectors II: the role of nanoparticle hydrophobicity. Langmuir 2011;27:11409–15. https://doi.org/10.1021/la202751y.

[45] Yang S, Pelton R, Montgomery M, Cui Y. Nanoparticle flotation collectors III: the role of nanoparticle diameter. ACS Appl Mater Interfaces 2012;4:4882–90. https://doi.org/10.1021/am301215h.

[46] Yang S, Razavizadeh BBM, Pelton R, Bruin G. Nanoparticle flotation collectors—the influence of particle softness. ACS Appl Mater Interfaces 2013;5: 4836–42. https://doi.org/10.1021/am4008825.

[47] Dong X, Marway HS, Cranston ED, Pelton RH. Relating nanoparticle shape and adhesiveness to performance as flotation collectors. Ind Eng Chem Res 2016;55: 9633–8. https://doi.org/10.1021/acs.iecr.6b02488.

[48] Dong X, Price M, Dai Z, Xu M, Pelton R. Mineral-mineral particle collisions during flotation remove adsorbed nanoparticle flotation collectors. J Colloid Interface Sci 2017;504:178–85. https://doi.org/10.1016/j.jcis.2017.05.050.

[49] Dong X, Gustafsson E, Price M, Dai Z, Xu M, Pelton R. Glass bead-bead collisions abrade adsorbed soft-shell polymeric nanoparticles leaving footprints. Colloids Surf A Physicochem Eng Asp 2017;533:159–68. https://doi.org/10.1016/j.colsurfa.2017.08.030.

[50] Yang S, Pelton R, Abarca C, Dai Z, Montgomery M, Xu M, et al. Towards nanoparticle flotation collectors for pentlandite separation. Int J Miner Process 2013;123:137–44. https://doi.org/10.1016/j.minpro.2013.05.007.

[51] Abarca C, Yang S, Pelton RH. Towards high throughput screening of nanoparticle flotation collectors. J Colloid Interface Sci 2015;460:97–104. https://doi.org/10.1016/j.jcis.2015.08.052.

[52] Zhou X, Feng B. The effect of polyether on the separation of pentlandite and serpentine. J Mater Res Technol 2015;4:429–33. https://doi.org/10.1016/j.jmrt.2015.02.002.

[53] An M, Liao Y, Gui X, Zhao Y, He Y, Liu Z, et al. An investigation of coal flotation using nanoparticles as a collector. Int J Coal Prep Utiliz 2020;40:679–90. https://doi.org/10.1080/19392699.2017.1402767.

[54] An M, Liao Y, Cao Y, Zhao Y, Qiu Y. Tetrahydrofurfuryl-functionalized polystyrene nanoparticles as collectors for low rank coal flotation. Physicochem Probl Miner Process 2019;55:516–27. https://doi.org/10.5277/ppmp18163.

[55] Liao Y, An M, Hao X, Song X, Yang Z, Ren H, et al. Enhanced floatability of low rank coal using surface functionalized polystyrene nanoparticles as collectors. J Clean Prod 2021;284:124763. https://doi.org/10.1016/j.jclepro.2020.124763.

[56] Liao Y, Ren H, An M, Zhao Y, Hao X. Mechanism of enhancing low rank coal flotation using nanoparticles as a novel collector. J China Coal Soc 2021;46: 2767–75.

[57] Fu L, Li W, Pan Z, Zhang Z, Jiao F, Qin W. Synthesis of modified polystyrene nanoparticles and their application in fine cassiterite flotation. Colloids Surf A Physicochem Eng Asp 2024;681:132608. https://doi.org/10.1016/j.colsurfa.2023.132608.

[58] He GC, Ding J, Huang CH, Kang Q. Synthesis of nanoparticle emulsion collector HNP and its application in microfine chalcopyrite flotation. IOP Conf Ser: Mater Sci Eng 2018;292:012029. https://doi.org/10.1088/1757-899x/292/1/012029.

[59] Murga R, Rodriguez C, Amalraj J, Vega-Garcia D, Gutierrez L, Uribe L. Use of polystyrene nanoparticles as collectors in the flotation of chalcopyrite. Polymers 2022;14:5259. https://doi.org/10.3390/polym14235259.

[60] Yang B, Liu J, Wang L, Ai G, Ren S. Enhanced collection of chalcopyrite by styrene-butyl acrylate polymer nanospheres in the presence of serpentine. Colloids Surf A Physicochem Eng Asp 2022;640:128408. https://doi.org/10.1016/j.colsurfa.2022.128408.

[61] Hartmann R, Beaumont M, Pasquie E, Rosenau T, Serna-Guerrero R. N-alkylated chitin nanocrystals as a collector in malachite flotation. ACS Sustain Chem Eng 2022;10:10570–8. https://doi.org/10.1021/acssuschemeng.2c01978.

[62] Hrůzová K, Matsakas L, Sand A, Rova U, Christakopoulos P. Organosolv lignin hydrophobic micro- and nanoparticles as a low-carbon footprint biodegradable flotation collector in mineral flotation. Bioresour Technol 2020;306:123235. https://doi.org/10.1016/j.biortech.2020.123235.

[63] Hrůzová K, Kolman K, Matsakas L, Nordberg H, Christakopoulos P, Rova U. Characterization of Organosolv lignin particles and their affinity to sulfide mineral surfaces. ACS Appl Nano Mater 2023;6:17387–96. https://doi.org/10.1021/acsanm.3c02069.

[64] Ai G, Liu C, Zhu G, Yang S. A nanoparticle cationic polystyrene-co-poly(n-butylacrylate) collector to eliminate the negative effect of lizardite slimes in pyrite flotation. Physicochem Probl Miner Process 2023;59:170899. https://doi.org/10.37190/ppmp/170899.

[65] Cheng G, Zhang J, Su H, Zhang Z. Synthesis and characterization of a novel collector for the desulfurization of fine high-sulfur bauxite via reverse flotation. Particuology 2023;79:64–77. https://doi.org/10.1016/j.partic.2022.11.012.

[66] Cheng G, Zhang J, Su H, Zhang Z. A novel collector for high-sulfur bauxite flotation desulfurization. Sep Sci Technol 2023;58:86–100. https://doi.org/10.1080/01496395.2022.2103000.

[67] Teotia AK, Sami H, Kumar A. Thermo-responsive polymers: Structure and design of smart materials. Switchable and responsive surfaces and materials for biomedical applications. Elsevier; 2015. p. 3–43.

[68] Sakohara S, Kawachi T, Gotoh T, Iizawa T. Consolidation of suspended particles by using dual ionic thermosensitive polymers with incorporated a hydrophobic component. Sep Purif Technol 2013;106:90–6. https://doi.org/10.1016/j.seppur.2012.12.030.

[69] Alarcón CDLH, Pennadam S, Alexander C. Stimuli responsive polymers for biomedical applications. Chem Soc Rev 2005;34:276–85. https://doi.org/10.1039/b406727d.

[70] Franks GV, Li H, O'Shea J-P, Qiao GG. Temperature responsive polymers as multiple function reagents in mineral processing. Adv Powder Technol 2009;20: 273–9. https://doi.org/10.1016/j.apt.2009.02.002.

[71] Burdukova E, Li H, Bradshaw DJ, Franks GV. Poly (N-isopropylacrylamide) (PNIPAM) as a flotation collector: effect of temperature and molecular weight. Miner Eng 2010;23:921–7. https://doi.org/10.1016/j.mineng.2010.03.003.

[72] Franks G, Forbes E, Li Ishida N, O'Shea. Mechanism responsible for flocculation in Poly-(N-Isopropylacrylamide) temperature responsive dewatering - Attractive interaction forces induced by surface hydrophobicity. 2010.

[73] Forbes E, Bradshaw DJ, Franks GV. Temperature sensitive polymers as efficient and selective flotation collectors. Miner Eng 2011;24:772–7. https://doi.org/10.1016/j.mineng.2011.02.003.

[74] Ng WS, Sonsie R, Forbes E, Franks GV. Flocculation/flotation of hematite fines with anionic temperature-responsive polymer acting as a selective flocculant and collector. Miner Eng 2015;77:64–71. https://doi.org/10.1016/j.mineng.2015.02.013.

[75] Ng WS, Connal LA, Forbes E, Franks GV. Xanthate-functional temperature-responsive polymers as selective flocculants and collectors for fines recovery. Miner Eng 2016;96-97:73–82. https://doi.org/10.1016/j.mineng.2016.05.013.

[76] Ng WS, Cooper L, Connal LA, Forbes E, Jameson GJ, Franks GV. Tuneable collector/depressant behaviour of xanthate-functional temperature-responsive polymers in the flotation of copper sulfide: effect of shear and temperature. Miner Eng 2018;117:91–9. https://doi.org/10.1016/j.mineng.2017.12.008.

[77] Chanturia VA, Matveeva TN, Ivanova TA, Getman VV. Mechanism of interaction of cloud point polymers with platinum and gold in flotation of finely disseminated precious metal ores. Miner Process Extr Metall Rev 2016;37:187–95. https://doi.org/10.1080/08827508.2016.1168416.

[78] Wang L, Lan H, Guan W, Wang Y, Han J, Yang Y, et al. New insights into selective flotation recovery of gold using dye-derived thermo-responsive polymeric surfactant: DFT calculation and adsorption mechanism. Sep Purif Technol 2023; 320:124199. https://doi.org/10.1016/j.seppur.2023.124199.

[79] Wang L, Liu Y, Liu Y, Mao Y, Han J, Li W, et al. Recyclable aptamer-derived aqueous two-phase flotation for high-efficiency separation of mercury(II) ions modulated by aggregation states. Sep Purif Technol 2021;274:118917. https://doi.org/10.1016/j.seppur.2021.118917.

[80] Zheng H, Zhang S, Yang C, Yin H, Liu W, Lu K. Simultaneous removal of Ni(II) and Cr(VI) from aqueous solution by froth flotation using PNIPAM-CS intelligent nano-hydrogels as collector. J Mol Liq 2021;342:117551. https://doi.org/10.1016/j.molliq.2021.117551.

[81] Xu J, Qiao H, Yu K, Chen M, Liu C, Richtering W, et al. Cu2+ tunable temperature-responsive Pickering foams stabilized by poly (N-isopropylacrylamide-co-vinyl imidazole) microgel: significance for Cu2+ recovery via flotation. Chem Eng J 2022;442:136274. https://doi.org/10.1016/j.cej.2022.136274.

[82] Mahmoud MR, Lazaridis NK. Simultaneous removal of nickel(II) and chromium(VI) from aqueous solutions and simulated wastewaters by foam separation. Sep Sci Technol 2015;50:1421–32. https://doi.org/10.1080/01496395.2014.978456.

[83] Lindman B, Alexandridis P. Amphiphilic molecules: Small and large. In: Alexandridis P, Lindman B, editors. Amphiphilic block copolymers. Amsterdam: Elsevier Science B.V; 2000. p. 1–12.

[84] Lockwood APG, Wadsley G, Warren NJ, Peakall J, Webber GB, Wanless EJ, et al. Amphiphilic block copolymers as dual flocculation-flotation agents for rapid solid–liquid separation of radioactive wastes. Sep Purif Technol 2023;323:124387. https://doi.org/10.1016/j.seppur.2023.124387.

[85] Saldívar-Guerra E, Vivaldo-Lima E. Introduction to polymers and polymer types. John Wiley & Sons, Inc.; 2013. p. 1–14.

[86] Xiong X, Wang J, Liu J, Xiao T. Microplastics and potentially toxic elements: a review of interactions, fate and bioavailability in the environment. Environ Pollut 2024;340:122754. https://doi.org/10.1016/j.envpol.2023.122754.

[87] Schild HG. Poly(N-isopropylacrylamide): experiment, theory and application. Prog Polym Sci 1992;17:163–249. https://doi.org/10.1016/0079-6700(92)90023-r.

[88] Ansari MJ, Rajendran RR, Mohanto S, Agarwal U, Panda K, Dhotre K, et al. Poly(N-isopropylacrylamide)-based hydrogels for biomedical applications: a review of the state-of-the-art. Gels 2022;8:454. https://doi.org/10.3390/gels8070454.